

1 This manuscript has been submitted for publication. Please feel free to contact any of the authors if  
2 you have any questions. Your feedback is very welcome.

3  
4  
5

## 6 **Keratose sponges in ancient carbonates – a problem of interpretation**

7

8 FRITZ NEUWEILER<sup>1</sup>, STEPHEN KERSHAW<sup>2\*</sup>, FRÉDÉRIC BOULVAIN<sup>3</sup>, MICHAŁ  
9 MATYSIK<sup>4</sup>, CONSUELO SENDINO<sup>5</sup>, MARK McMENAMIN<sup>6</sup>, RACHEL WOOD<sup>7</sup>

10

11 <sup>1</sup>*Département de géologie et de génie géologique, 1065, av. de la Médecine, Québec*  
12 *(Québec), G1V 0A6, Canada*

13 <sup>2</sup>*Department of Life Sciences, Brunel University, Uxbridge, UB8 3PH, UK; and Earth*  
14 *Sciences Department, The Natural History Museum, Cromwell Road, London SW7 5BD,*  
15 *UK (E-mail: [stephen.kershaw@brunel.ac.uk](mailto:stephen.kershaw@brunel.ac.uk))*

16 <sup>3</sup>*Pétrologie sédimentaire, Quartier Agora, B20, Allée du six Août, 12, Université de Liège,*  
17 *Sart Tilman, B-4000 Liège, Belgium*

18 <sup>4</sup>*Institute of Geological Sciences, Jagiellonian University, Gronostajowa 3a, 30-387,*  
19 *Kraków, Poland*

20 <sup>5</sup>*Earth Sciences Department, The Natural History Museum, Cromwell Road, London SW7*  
21 *5BD, UK*

22 <sup>6</sup>*Department of Geology and Geography, Mount Holyoke College, 50 College Street,*  
23 *South Hadley, Massachusetts 01075, USA*

24 <sup>7</sup>*School of Geosciences, Grant Institute, University of Edinburgh, Kings Buildings, James*  
25 *Hutton Road, Edinburgh, EH9 3FE, UK*

26

27 \*Corresponding author

28 <https://orcid.org/0000-0003-1099-9076> (S Kershaw)

29

30 Associate Editor – to be added by editors

31

32

## 33 **ABSTRACT**

34

35 Increasing current interest in sponge fossils includes numerous reports of diverse  
36 vermicular and peloidal structures interpreted as keratose sponges in Neoproterozoic to  
37 Mesozoic carbonates and in various open marine to peritidal and restricted settings.  
38 Reports of their occurrence are fundamental and far-reaching for understanding  
39 microfacies and diagenesis where they occur; and fossil biotic assemblages, as well as  
40 wider aspects of origins of animals, sponge evolution/ecology and the systemic recovery  
41 from mass extinctions. Keratose sponges: 1) have elaborate spongin skeletons but no  
42 spicules, thus lack mineral parts and therefore have poor preservation potential so that  
43 determining their presence in rocks requires interpretation; and 2) are presented in  
44 publications as interpreted fossil structures almost entirely in two-dimensional (thin  
45 section) studies, where structures claimed as sponges comprise diverse layered, network,  
46 particulate and amalgamated fabrics involving calcite sparite in a micritic groundmass.  
47 There is no verification of sponges in these cases and almost all of them can be otherwise  
48 explained; some are certainly not correctly identified. The diversity of structures seen in  
49 thin sections may be reinterpreted to include: a) meiofaunal activity; b) layered, possibly

50 microbial (spongiostromate) accretion; c) sedimentary peloidal to clotted micrites; d) fluid  
51 escape and capture resulting in birdseye to vuggy porosities; and e) molds of siliceous  
52 sponge spicules. Without confirmation of keratose sponges in ancient carbonates,  
53 interpretations of their role in ancient carbonate systems, including facies directly after  
54 mass extinctions, are unsafe, and alternative explanations for such structures should be  
55 considered. This study calls for greater critical appraisal of evidence, to seek confirmation  
56 or not, of keratose sponge presence.

57 (259/300 max, for Sedimentology)

58

59 **Keywords** Carbonate rock, sponge, microfabric, spongiostromate, birdseyes, meiofauna,  
60 metazoan evolution.

61

62

### 63 INTRODUCTION AND AIM

64 This study addresses the issue of recognition of keratose sponges in thin sections of  
65 carbonate rocks, important because claims of their preservation potentially extends the  
66 body fossil record deep into the Neoproterozoic (Turner, 2021), thereby affecting analysis  
67 of sedimentary facies containing these structures across a long time range. For the  
68 purposes of our investigation, sponges present two fundamental forms that require  
69 understanding in relation to their preservation as fossils: 1) those with mineral spiculate  
70 skeletons (Figs 1E, F, 2A, B, 3, 4A-D) versus 2) those lacking such mineral parts (Fig. 1A-  
71 D, 2C, D, 4E-F), the latter constituting the Keratosa group of demosponges (Fig. 5). The  
72 taxonomic status of the best-known fossil aspiculate sponge *Vauxia*, examples of which  
73 are shown in Fig. 4E-F, is unconfirmed (Ehrlich *et al.*, 2013). Sponges with mineral  
74 spiculate skeletons are most easily studied in hand specimens (e.g. Botting *et al.*, 2017,  
75 Rigby *et al.*, 2008) as either whole fossils, or as disaggregated spicules, noting that on  
76 death sponges generally break up very quickly, spicules readily dissolve and normally  
77 disappear to leave no record (Debrenne, 1999; Wulff, 2016). Thus, knowledge of the  
78 geological history of sponges has relied greatly on molecular clock phylogeny (e.g.  
79 Schuster *et al.* 2018; Kenny *et al.* 2020), see Fig 5. Fossil sponges with mineral skeletons,  
80 where preserved, are thus relatively easily recognizable in hand specimens but in thin  
81 sections are open to some interpretation, particularly if disaggregated (see Flügel, 2004, p.  
82 495, 799). However, keratose sponges are significantly more problematic, yet have been  
83 inferred in a range of facies in the rock record, addressed next.

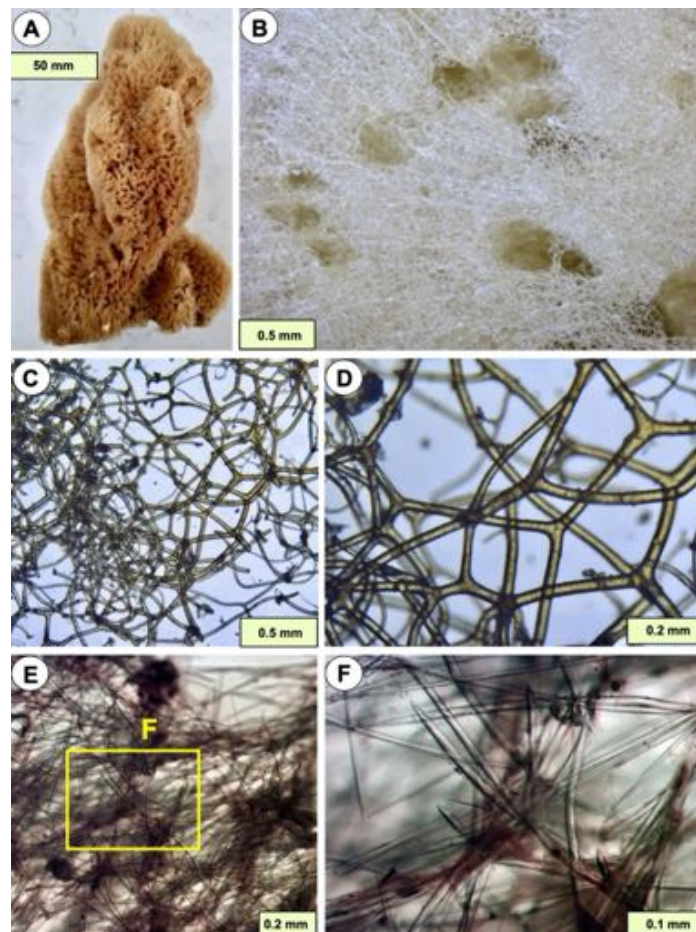
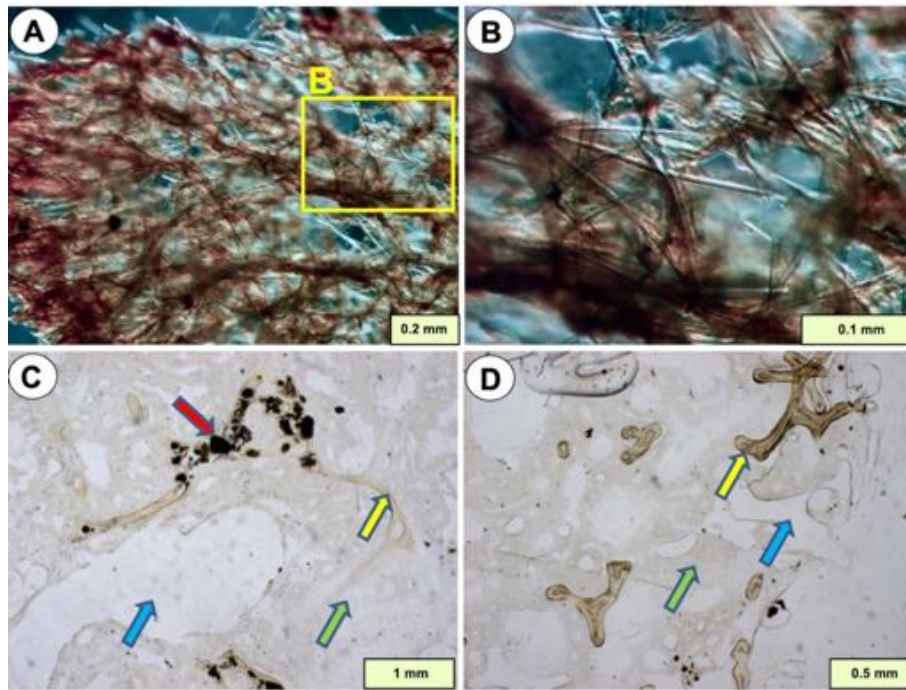


**Figure 1** – Examples of modern sponges showing contrasting construction of spiculate and keratose sponges. (A) Side view of a modern commercial keratose sponge consisting of only spongin (all the soft tissue is removed) showing its form is maintained by the spongin network. (B) Detail of sponge surface showing the spongin network and oscula (large holes) accommodating the excurrent canal system, a feature missing in the reported cases of fossil interpreted keratose sponges. (C-D) Details of the branched nature of the spongin network in A, showing branches and curved features; note that if ancient carbonate structures illustrated in this study, and references herein, represent keratose sponges, then the spongin networks shown in these two photographs would need to be preserved as calcite and the intervening empty space occupied by micrite. (E-F) Details of spiculate structure of *Phakellia robusta* Bowerbank, Shetland, Scotland. Bowerbank collection, Natural History Museum, London, sample, NHMUK 1877.5.21.420.

84  
85  
86  
87  
88  
89  
90  
91  
92  
93  
94  
95



96  
97  
98  
99  
100  
101  
102  
103  
104  
105  
106  
107  
108

**Figure 2** – Examples of two modern sponges demonstrating more diversity of sponge architecture relevant to this study. (A, B) *Axinella verrucosa* [should be Esper but the label appears to say "Schmidt"], from the Adriatic Sea, showing spongin fibres encrusted by spicules; if the spongin component is to be preserved as a fossil, then it may be expected that sponges comprising both spongin and spicules should show both components in the fossil record, and this has not yet been demonstrated, see text for discussion. Bowerbank collection, Natural History Museum, London, sample NHMUK 1877.5.21.1239. (C, D) *Ircinia keratose* sponge showing strong primary spongin fibres (yellow arrow), soft porous mesohyl tissue (green arrow) with water canals (blue arrow), and incorporated detrital particles (red arrow, common in sponges). Joulters Cay, Bahamas.

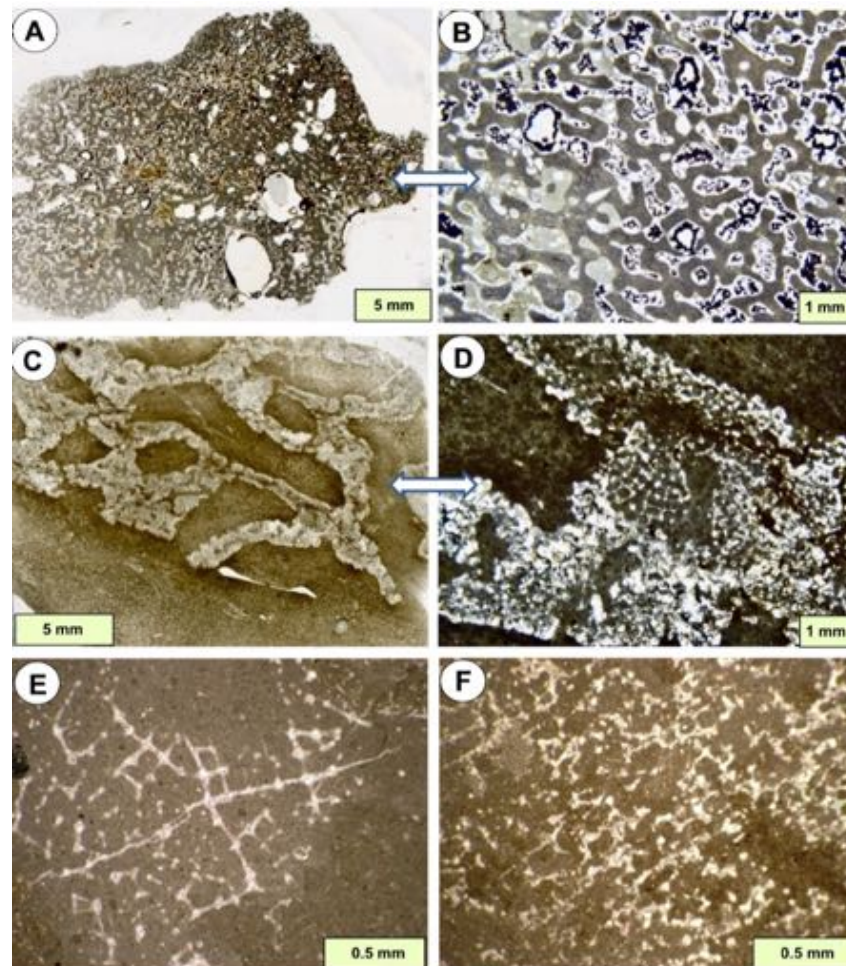


**Figure 3** – Examples of sponge mummies. (A, B) Calcified Cretaceous sponge from the Faringdon gravels, England, showing the sponge structure preserved as calcite and infilled with micrite. (C, D) Calcified Cretaceous sponge from the Chalk Group, Beachy Head, Eastbourne, England, showing a partially preserved spiculate network. (E) Hexactinellid sponge mummy showing details of spicule network preservation as calcite. (F) Lithistid sponge showing desma spicules preserved in calcite. E and F from Dalichai Formation, Bajocian-Calloviaian (Jurassic), Alborz Mountains, northern Iran. Photographs kindly provided by Andrej Pisera.

109  
110  
111  
112  
113  
114  
115  
116  
117  
118

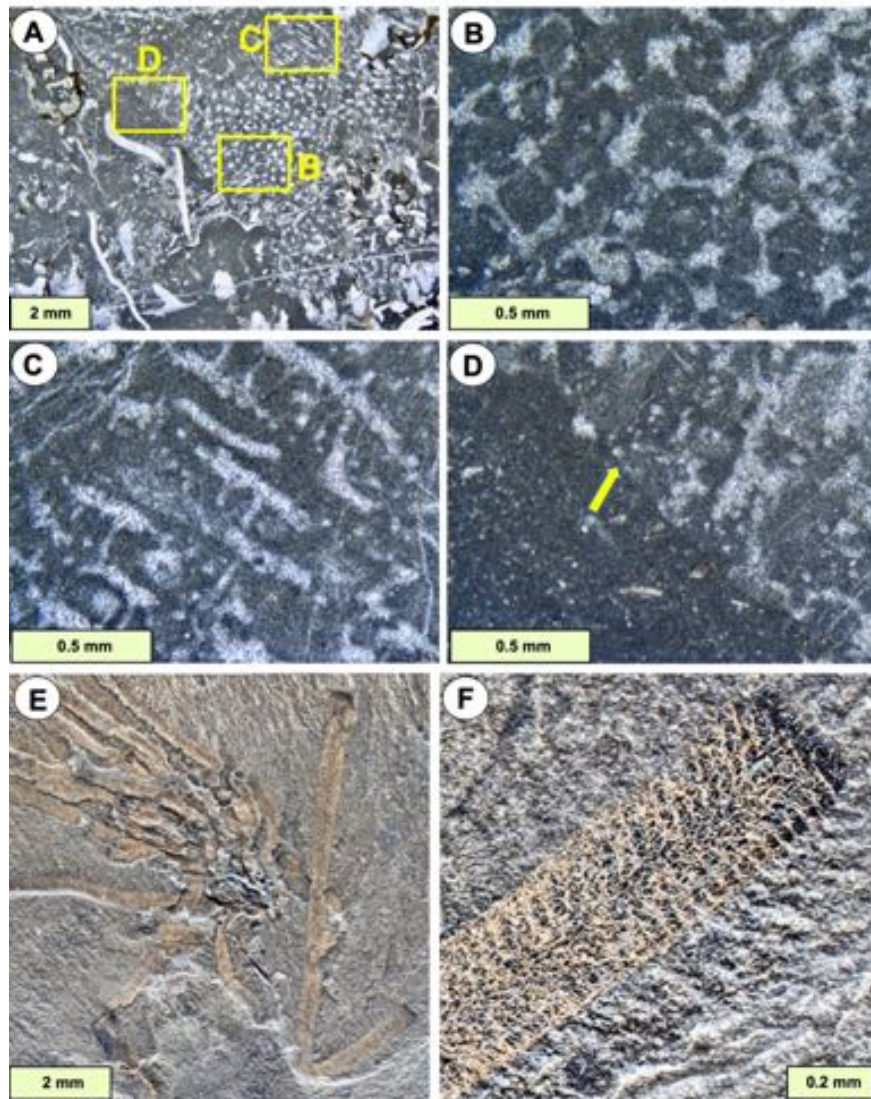


**Figure 4** – (A-D) Calcified spiculate sponges, may be lithistids, showing the rectilinear network structure described in the text. (A) the sponge forms a discrete object in the upper right half, locations of B-D are indicated. (B-C) Details of transverse (B) and vertical (C) sections of spiculate structure, noting spicules are preserved as calcite. (D) Detail of margin of sponge showing its sharp contact (arrow) with surrounding micrite. Church Reef, Filimore Formation, L. Ordovician, Utah. (E, F) The aspiculate fossil sponge *Vauxia gracilenta* Walcott, 1920 from the Burgess Shale, regarded as one of the best examples of aspiculate, possibly Keratose sponges, see Walcott (1917). Specimen NHMUK PI S3071 in the Natural History Museum, London.

119  
120  
121  
122  
123  
124  
125  
126  
127  
128  
129  
130

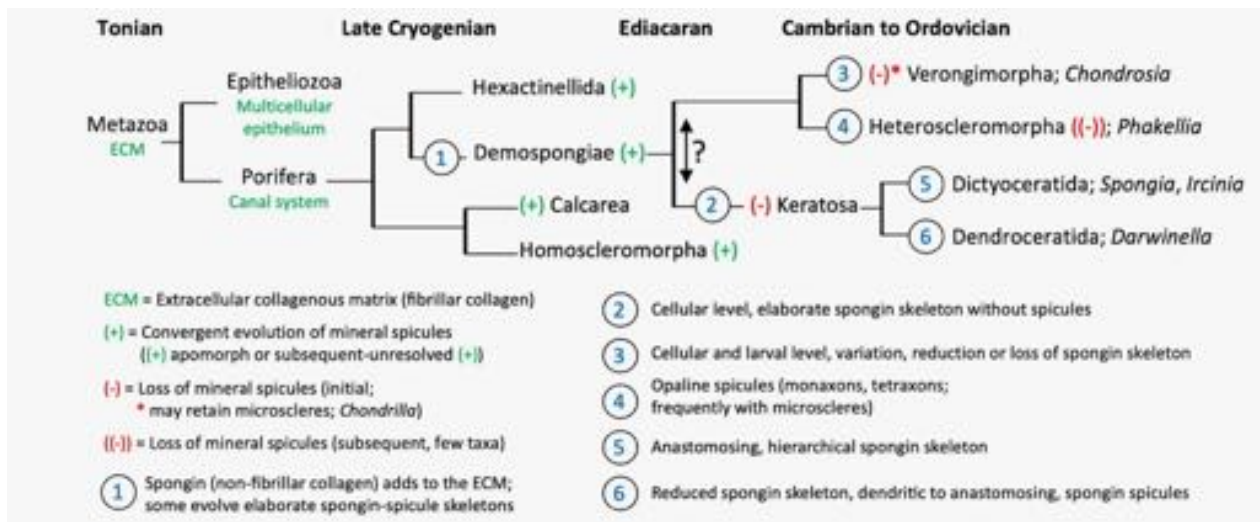
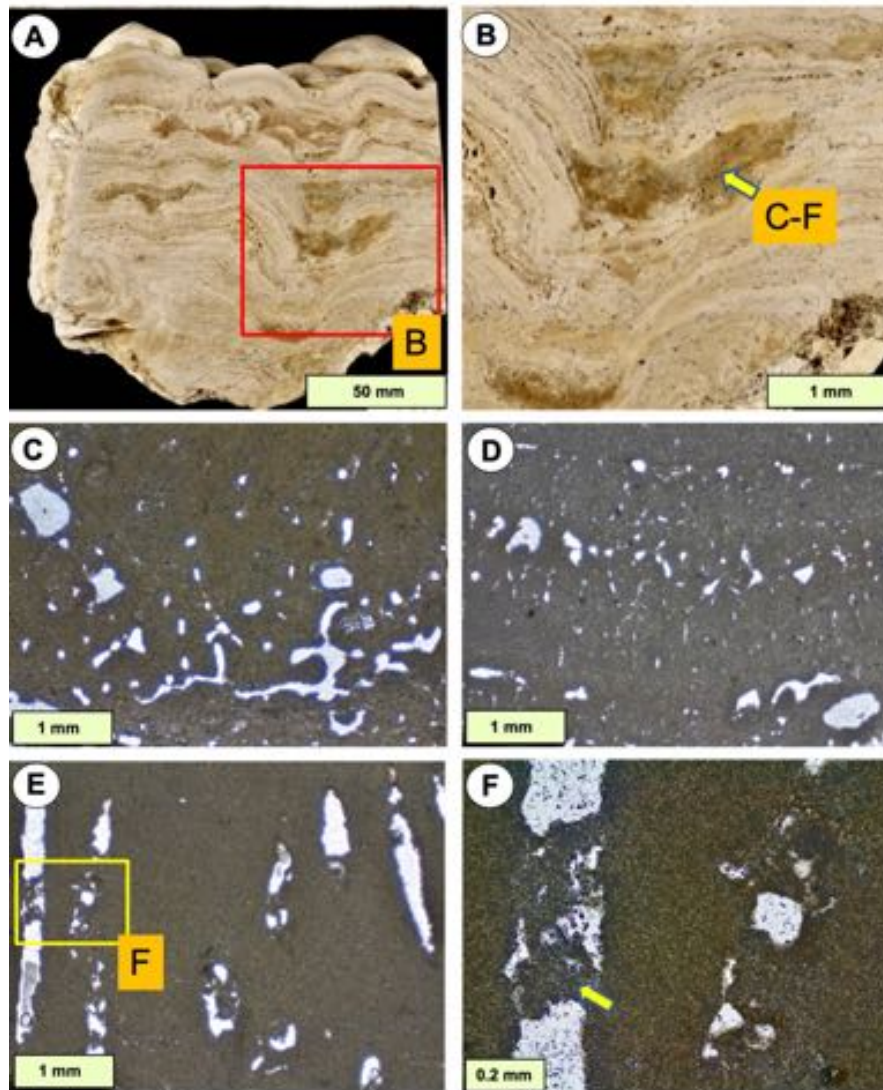


**Figure 5** – Summary evolutionary history of sponges (see Schuster *et al.* 2018; Kenny *et al.* 2020), drawing attention to major events including the origin of the Keratosa, that are the principal subject of this paper.

131  
132  
133  
134  
135  
136  
137  
138  
139  
140  
141  
142

The origin of interpretations of fossil keratose sponges in carbonates seems to have been a study by Szulc (1997) who described stromatolites from restricted lagoonal facies (Matsyik, 2016) in the Middle Triassic Muschelkalk carbonates from Upper Silesia; Szulc inferred that pockets and layers of porous micrite within the stromatolites are sponges (Fig. 6).



143  
144 **Figure 6** – Stromatolite samples proposed by Szulc (1997) to contain sponges. (A, B) Vertical sections  
145 through stromatolite showing interlayered sediment in which the porous fabrics (yellow arrow) occur that  
146 were considered as sponge by Szulc. (C, D) Vertical thin section views of the interlayered sediment in A, B,  
147 showing organised porosity as subvertical voids. (E, F) Detail of one pore, showing partial infill with micrite  
148 (yellow arrow), evidence that the pore must have been open to the sea floor to collect sediment and thus not  
149 consistent with interpretation as a permineralised sponge. From the collections of Joachim Szulc; boundary  
150 between *Diplora* Beds and overlying Tarnowice Beds, Muschelkalk, Middle Triassic, Libiąż Quarry, Upper  
151 Silesia, Poland.

152

153

154

155

156

157

158

159

160

161

162

163

164

However, Szulc (1997, p. 14) did not give criteria for recognition of sponges, the porous  
vermicular structures he described have no spicules (Fig. 6) and are preserved in  
dolomite. Also there is an issue regarding the likelihood of occurrence of sponges in  
combination with stromatolites in restricted facies, not known in modern environments.  
Confusingly Szulc (1997) noted similar deposits from Thuringia that are silicified, from  
which he inferred the proposed sponges were siliceous, but without any supporting  
evidence. Non-spiculate sponges were similarly inferred by Reitner *et al.* (2001) and  
Reitner & Wörheide (2002, fig. 10) for Devonian mud-mounds. Then, in a landmark study,  
Luo & Reitner (2014) used serial grinding and imaging methods to construct 3D views,  
leading to their interpretation of possible fossil keratose sponges (aspiculate) to explain



165 vermicular structure in other carbonates. However, their reconstructions were inconclusive,  
166 with their original interpretation unsubstantiated, as recognized by Luo & Reitner (2014)  
167 themselves, who used terms such as “most likely”, “putative” and “preliminary”.  
168 Subsequently, Luo & Reitner’s (2014) work was developed by Luo & Reitner (2016), then  
169 these studies were used to support numerous claims of keratose sponges in other  
170 carbonates from Neoproterozoic to at least Triassic time (see compilation of publications in  
171 Table S1), without verification, and no others have attempted 3D reconstruction. Instead,  
172 evidence is presented in 2D images (thin sections), commonly at low-resolution where  
173 details are not clear, and rely on broad textural features as the basis of a sponge  
174 interpretation.

175 Thus the problem that keratose sponges present is lack of reliable identification of  
176 their fossilized remains in any part of the rock record; and there is no known diagenetic  
177 process that could transform the entity of the porous soft tissue (between the spongin  
178 fibres, see Fig. 2C, D) into the largely homogenous micrite that dominates interpreted  
179 keratosaurs. In contrast, Figs. 3 and 4 show the types of preservation of fossil sponges  
180 commonly encountered in thin section, that, with the exception of Fig. 4E & F, comprise  
181 mineral parts. Therefore, this study draws attention to the difficulties of understanding the  
182 fabrics of interpreted keratose sponges in carbonate rocks that may instead be viewed  
183 diversely as *Problematica* (definite fossils, the affinities of which are not known), fragments  
184 of altered siliceous sponges, graphoglyptid trace fossils or even dubiofossils. Thus, the  
185 aim of this study is to bring into focus the problem of recognition of keratose sponges, and  
186 consider alternatives that may be explored in future research. In order to explain the  
187 issues fully, a background review is provided of the issues around fossil sponges that  
188 necessarily involves description of relevant features of modern sponges. Then  
189 classification, description and discussion of the range of fabrics of carbonate rocks  
190 published as interpreted keratose sponges is presented, relevant to microfacies analysis of  
191 carbonate rocks. The focus is on four key settings in which keratose sponges have been  
192 interpreted: Neoproterozoic carbonates, consortia between stromatolites and sponges  
193 (especially Triassic), Cambro-Ordovician carbonates, and carbonate facies in the  
194 aftermath of mass extinctions.

195  
196

## 197 **BACKGROUND**

198 Ambiguities in the interpretation and thus classification of sedimentary carbonate materials  
199 are widespread; such ambiguities are mostly related to the structure and volumetric  
200 importance of relatively small microcrystalline grains (Lokier & Al Juanabi, 2016). Sources  
201 of error include the problems of identification, in thin-section, of structures that may be  
202 fossils, in terms of form, functional design and skeletal microstructure (Knoll, 2003; Flügel  
203 and Munnecke, 2010), thus constituting a grey zone between clearly identifiable and  
204 suspect structures. This grey zone comprises objects that may be considered in three  
205 types: a) biogenic but require interpretation in terms of basic taxonomic placement  
206 (*Problematica sensu lato*; Jenner & Littlewood, 2008; e.g. Paleozoic *Halysis* as red alga,  
207 cyanobacteria, green alga or tabulate coral; Zheng *et al.*, 2020), b) distinct structures but  
208 inconclusive in terms of biogenicity (dubiofossils of Hofmann, 1972), and c) distinct  
209 structures that are certainly abiotic in nature (pseudofossils, full discussion in McMahon *et*  
210 *al.*, 2021). Another aspect is that the granularity of carbonate deposits does not  
211 necessarily relate to sedimentary processes; it might be post-depositional in nature due to  
212 meio- to endofaunal activity, localized microburrow nests or even diagenesis (Debrenne *et*  
213 *al.*, 1989; Wood *et al.*, 1993; Pemberton & Gingras, 2005; Löhr & Kennedy, 2015;  
214 McMenamin, 2016; Wright & Barnett, 2020). Furthermore, this grey zone applies to cases  
215 that extend into deep time and even touches exobiology (Cloud, 1973; e.g., biogenicity

216 criteria for tubular filaments and lamination; chemical gardens comprising inorganic  
217 processes resulting in structures resembling organisms; molar-tooth structures; see  
218 Grotzinger & Rothman, 1996; Awramik & Grey, 2005; McMahon *et al.*, 2017, 2021;  
219 McMahon & Cosmidis, 2021). This range of fabrics persists throughout the Phanerozoic in  
220 various ways; examples are: the biogenicity of stromatactis and lamination (Bathurst,  
221 1982; Bourque & Boulvain, 1993; Awramik & Grey, 2005; McMahon *et al.*, 2021); the  
222 formation of peloids (Macintyre, 1985); the significance of the polymud fabric (Lees &  
223 Miller, 1995; Neuweiler *et al.*, 2009); or some drag marks, *Rutgersella* and *Frutexites*  
224 (Cloud, 1973; Retallack, 2015; McMahon *et al.*, 2021).

225 During the last decade, molecular phylogenetic studies have shed new light  
226 on the traditional taxonomic and phylogenetic framework of sponges, revealing or  
227 confirming several polyphyletic groups, establishing new clades, and constraining  
228 respective divergence-time estimates (Gazave *et al.*, 2012; Erpenbeck *et al.*, 2012;  
229 Morrow & Cárdenas, 2015; Schuster *et al.*, 2018; Kenny *et al.*, 2020), see Fig. 5. A  
230 valuable general reference for sponge groups is de Voogd *et al.* (2022). Spongin is  
231 considered to have evolved in tight connection within the demosponge lineage (Morrow &  
232 Cárdenas, 2015). Sponge spicules may not represent an essential character of early  
233 sponge evolution (Ax, 1996), and were secondarily lost in a multiple and convergent  
234 manner (Fig. 5). Keratose sponges are distinguished from other aspiculate demosponges  
235 (Verongimorpha, some Heteroscleromorpha according to Erpenbeck *et al.*, 2012) at the  
236 cellular level in combination with the details or even absence of an elaborate spongin  
237 skeleton (Erpenbeck *et al.*, 2012).

238 As indicated in the Introduction, the secure identification of fossil sponges  
239 essentially relies on spicules, commonly identified according to their specific design and  
240 arrangement, comprising: form, orientation; assemblage and mineralogy (examples in Figs  
241 1-4). Sponge form may also be preserved *via* a process referred to as mummification, that  
242 is early calcification (thus lithification) of the sponge tissue with its associated sediment, to  
243 preserve the sponge shape and organisation sufficiently enough to allow recognition as a  
244 sponge (canal system, preservation of non-rigid spicular architecture; Fritz, 1958; Bourque  
245 & Gignac, 1983; Reitner & Keupp, 1991; Pisera, 1997; Neuweiler *et al.*, 1999; Reitner &  
246 Wörheide, 2002; Neuweiler *et al.*, 2007 with references therein). In other cases, there are  
247 specific secondary calcareous skeletons that leave a good record, preserved as, e.g.,  
248 stromatoporoids, chaetetids, inozoans and sphinctozoans, at least one of which  
249 (*Vaceletia*) is considered a coralline keratose sponge (Wörheide, 2008). Some sponges  
250 leave distinct ichnofossils (*Entobia*), that may contain spicule evidence of their formation  
251 (Reitner & Keupp, 1991, Bromley & Schönberg, 2008). Biomarkers might be of additional  
252 value (e.g. Love *et al.* 2009; see also Antcliffe *et al.*, 2014), but their study requires a  
253 detailed understanding of both history of fluid flow and molecular analogues of possible  
254 other origin. Confusingly, some foraminifera use sponge spicules to agglutinate their tests  
255 (Ruetzler & Richardson, 1996; Kamenskaya *et al.*, 2015) and thus need careful study to  
256 distinguish them from sponges.

257 Against the background of well-known modern aspiculate sponges (Keratosa and  
258 Verongimorpha) with their enormous architectural variability (Manconi *et al.*, 2013;  
259 Stocchino *et al.*, 2021), the situation is naturally precarious for claims of fossil non-coralline  
260 keratose demosponges to be preserved in limestones and dolostones. The body shape  
261 stability of keratose sponges (Fig. 1A, B) relies on fibrillar collagen as a key component of  
262 their extracellular collagenous matrix (ECM), that at micro- to macroscale is combined with  
263 a highly elastic and elaborate organic skeleton composed of the non-fibrillar collagen  
264 spongin (Exposito *et al.*, 1991; Erpenbeck *et al.*, 2012; Ehrlich, 2019). Indeed, the fossil  
265 record of non-spiculate sponges was described by Reitner & Wörheide (2002) as being  
266 poor, noting that the vauxiid sponges of the middle Cambrian Burgess Shale are the best

267 examples (Fig. 4E, F). However, Ehrlich *et al.* (2013) revealed that those sponges contain  
268 chitin (as other sponges and a number of invertebrates do), but not spongin. Fan *et al.*  
269 (2021) classified aspiculate vauxiid sponges in the Chengjiang biota (early Cambrian) as  
270 keratose sponges, preserved in partly silicified form.

271 Apart from vauxiids noted above, in literature search no verified cases of keratose  
272 sponges have been found in the entire rock record. An important aspect is that, within  
273 modern spiculate sponges, there are variable amounts of non-spicular material in  
274 proportion to the spicule content. Thus, it is necessary to appreciate the detailed features  
275 of sponges with and without spicules. Fig. 2A, B shows details of a modern  
276 heteroscleromorph spiculate demosponge that has spongin fibres encrusted with opaline  
277 spicules, and is one example of the common occurrence of tightly connected spicules and  
278 spongin fibres known for many decades (Axinellidae Carter, 1875), yet there is no report of  
279 a respective thin-section fossil that replicates such a distinct composite skeletal  
280 architecture. Singular claims for fossil Axinellidae are unconfirmed (Reitner & Wörheide,  
281 2002, their Fig. 9, which may instead be spicule-preserving *Entobia*). In addition there are  
282 modern non-spiculate (keratose) sponges comprising conspicuous primary fibres of  
283 spongin up to 250  $\mu\text{m}$  thick and distinctively cored by sand grains (Irciniidae, Gray 1867;  
284 see also Manconi *et al.*, 2013) (Fig. 2C, D) but again, there is no fossil record. For further  
285 comparison, Figs 3 and 4A-D demonstrate carbonate fabrics typical of preserved spicule-  
286 bearing sponges, but in these there is no indication of the spongin component that is  
287 presumed lost in decay and diagenesis. Such details are important to gain an  
288 understanding of how such soft-tissue structures might be preserved, and comparisons  
289 between these and fossil cases are made later in this paper. Nevertheless, prominent  
290 examples of interpreted keratose sponges are in studies by Luo & Reitner (2016), Lee &  
291 Hong (2019), Lee & Riding (2021a, b), Baud *et al.* (2021), Pei *et al.* (2021), Pham *et al.*  
292 (2021), Gischler *et al.* (2021) and Turner (2021). None of those studies highlighted  
293 biostratinomy in combination with porosity evolution and diagenesis. Criteria for  
294 distinguishing, for example, carbonate microfibrils attributed to sponges from microbial  
295 deposits in ancient carbonates (Wallace *et al.*, 2014; Shen & Neuweiler, 2018) are not  
296 defined, and there are numerous other possible interpretations that are explored in this  
297 study.

298  
299

## 300 MATERIAL AND METHODS

301 In order to address the ideas regarding keratose sponges in the carbonate rock record, a  
302 range of samples from was used: Cambrian of North China, Cambro-Ordovician of Nevada  
303 and Utah, Silurian of south China, Devonian of Belgium, Viséan of Boulonnais region  
304 (France) and Triassic of the Upper Silesian region (Poland) including some original  
305 samples from the Triassic material from Poland and Israel used by Szulc (1997) and Luo &  
306 Reitner (2014, 2016). For basic reference, examination was made of the original  
307 spongiostromate material (Visé Group, Namur region) of Gürich (1906) stored at the Royal  
308 Belgian Institute of Natural Sciences (Brussels) and a selection of modern spiculate and  
309 non-spiculate sponges illustrated by: Bowerbank (1862) stored at the Natural History  
310 Museum London (UK); and from personal collections of the authors. Some published  
311 figures are reproduced under Creative Commons licences. Polished rock samples and thin  
312 sections were studied under plane-polarised (PPL) and cross-polarised (XPL) light,  
313 supplemented with selected cathodoluminescence (CL) and UV fluorescence views.

314  
315

316

## 317 RESULTS

318 In an attempt to follow the history of this topic, examination was made of Szulc's (1997)  
319 sample material of stromatolitic deposits stored in the Jagellonian University, Poland,  
320 illustrated here with new thin sections and cathodoluminescence; then the study was  
321 developed to address other structures claimed as keratose sponges. Perusal of the  
322 literature and primary material led to recognition that structures interpreted as fossil  
323 keratose sponge may be divided into five broad fabric types differing in context,  
324 architecture and microstructure. Some overlap occurs between the five categories, thus  
325 some examples presented here may fit into more than one type. All are based on two-  
326 dimensional views in thin sections. All are composed of areas of sparite intermingled with  
327 micritic material, the latter commonly comprising homogenous micrite, but in some cases  
328 showing clotted to granular fabrics. In some other cases reported in literature, they occur  
329 within shells but not in the matrix surrounding the shells (Park *et al.*, 2017, fig. 3); in still  
330 other cases they occur in discrete patches in micrite, and may have been burrows (Park *et*  
331 *al.*, 2015, fig. 4D); these two cases may reflect re-burrowing of organic-rich sediment  
332 encased in pre-existing burrows and shells. Many other examples occur within early-  
333 formed cavities in early-lithified limestone (Lee *et al.*, 2014). Some of the micritic material  
334 contains fossils (e.g. Lee & Hong, 2019, fig. 2c) which are difficult to explain if these were  
335 keratose sponges.

336 In Figs 6-17, according to the ideas of keratose sponge interpretation, the curved  
337 and irregular sparite patches represent the position of the original spongin structure and  
338 the micrite infill represents where the sponge soft tissue was located. Clearly, of great  
339 importance is to explain how: a) keratosan sponges could be preserved through a  
340 biostratinomic and diagenetic process that began with an elaborate organic skeleton made  
341 of spongin enveloped by a canal-bearing soft tissue and ended with sparitic calcite in a  
342 microcrystalline groundmass that comprises these fabrics; and b) if spongin components  
343 are present in fossils, why are they not visible along with spicule remains in spiculate  
344 sponges in at least some cases (c.f. Fig. 2A,B)?

#### 345 346 **Layered fabrics**

347 Within the Triassic stromatolites regarded by Szulc (1997) as containing sponges (Figs 6,  
348 7), the possible sponge component forms faint to prominent micrite layers containing  
349 porous network fabrics. Luo & Reitner (2014) used material from the same horizons.  
350

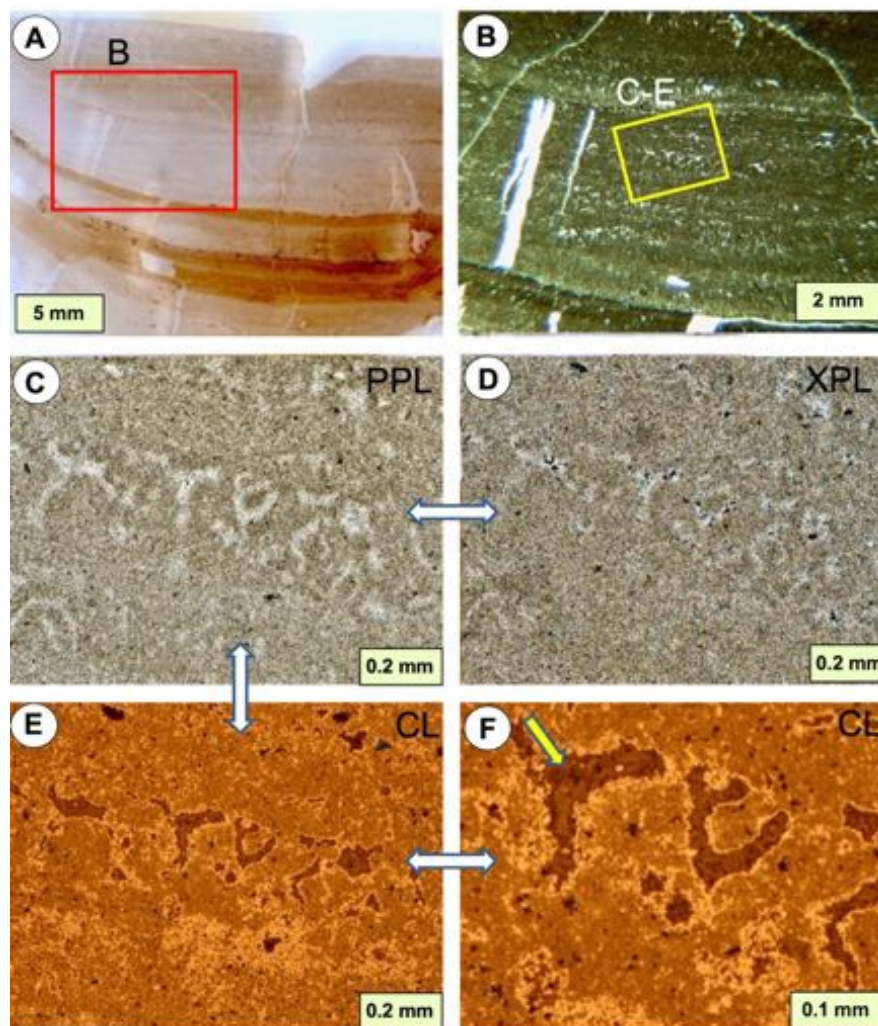


**Figure 7** – Vertical sections from a stromatolitic horizon, containing vermicular structures. (A) Whole thin section, showing prominent layered structure. (B) Detail of box in A, showing locations of C-F. (C, D) PPL (C) and XPL (D) views of vermicular structure within the stromatolite layers, showing sparite cement in the light areas. (E, F) CL view of C and D, with enlargement in F, showing a sequence of dull to no luminescence in the sparite areas (arrow), while the micrite areas contain a mixture of bright and dull luminescence. Note that the edges of the micrite against the sparite shows a higher degree of brighter luminescence. This pattern is interpreted to indicate that the sparite areas were vacated and infilled with cements, thus showing difference in diagenetic history from the micrite. From the collections of Joachim Szulc, sampled by him from the Ladinian (late Middle Triassic), Negev area, Israel.

351  
352  
353  
354  
355  
356  
357  
358  
359  
360  
361  
362

363 Layers in these materials broadly match the concept of spongiostromates, introduced by  
364 Gürich (1906) to convey their open architecture and layered bioaccretionary character  
365 (Figs 7, 8). The spongiostromate microstructure represents a microporous fabric of likely  
366 microbial accretion, generally blurred, grumelous to peloidal, at best faintly tubular to  
367 cellular/vesicular. This is in opposition to the porostromate microstructure that displays  
368 well-defined micro-organismic outlines preserved in growth position (Monty, 1981; for  
369 comparison, see Turner *et al.*, 2000; Flügel, 2004, p. 122). In this context layers comprise  
370 micrite normally enclosing somewhat irregular areas of sparite (Fig. 7), although some  
371 have open pores and others with micrite in the pores (e.g. Fig. 6F); the micrite may also  
372 include small bioclasts. Spongiostromate structures present a problem of interpretation  
373 because they have a spongy-looking fabric, in the common-English understanding of the  
374 term sponge, but without indication of a biological sponge nature, noting that Gürich's  
375 (1906) monograph illustrations obviously do not show sponges. The oldest known  
376 occurrences of spongiostromate structures forming part of oncoids reach back to the

377 Palaeoproterozoic (Schaefer *et al.*, 2001; Gutzmer *et al.*, 2002). Examples of  
378 spongiostromate-style fabrics interpreted to be keratose sponges may be seen in Luo &  
379 Reitner (2014, 2016), Pei *et al.* (2021a, b) and Lee & Riding (2021a, b). Stock & Sandberg  
380 (2019) illustrated layered fabrics of spongiostromate form in Devonian-Carboniferous  
381 boundary facies in Utah, which were presented as sponges, but their photographs are not  
382 sufficiently detailed to show structure that can be verified as sponge or not.

383 Layered fabrics may also show characters commonly described as birds-eyes,  
384 (connected) vugs and fenestrae, that are normally recognized as part of an intertidal to  
385 backreef carbonate system where degassing occurs in sediments exposed at the surface  
386 or in very shallow water (e.g. Tucker & Wright, 1990). They represent fabric-selective  
387 primary porosities with original voids commonly larger than the mean grain diameter.  
388 Laminae and sheets containing fabrics that may be reasonably interpreted as such,  
389 altogether being part of Triassic (Anisian) microbialites/stromatolites, were considered to  
390 be keratose sponges by Luo & Reitner (2014, 2016). In a subsequent step, the  
391 interpretation was developed to propose a distinction between a stromatolite and a  
392 sponge-microbial 'consortium' called keratolite by Lee & Riding (2021a). Conventionally,  
393 such structures are understood to form *via* the entrapment of gas bubbles, anhydrite  
394 precipitation and desiccation frequently in combination with dissolution and subsequent  
395 compaction in peritidal to intertidal (microbial) environments (Shinn, 1968). More recently,  
396 Bourillot *et al.* (2020) provided more details and a number of distinguishing parameters  
397 indicating how these porous microbialites/stromatolites may form their laminated-micritic,  
398 laminated-peloidal microfabrics.

399 Layered fabrics shown in Figs 7 and 8 compare plane light views with CL in paired  
400 images; the CL views show a cement stratigraphy in the sparitic areas, indicating void  
401 filling by a sequence of cement precipitation. The CL views show variation in cement  
402 history, with bright and dull luminescent cements occurring at different stages in the  
403 history. A common interpretation is that bright cement represents early burial low-oxygen  
404 conditions where bacterial sulfate reduction (BSR) removes iron from the porewaters  
405 precipitated as pyrite, so that manganese causes bright luminescence; later, below the  
406 zone of BSR, iron adds to the cement to quench the CL resulting in dull images (Scoffin,  
407 1987). This sequence can be envisaged in Fig. 7F, although Fig. 8 shows a different  
408 sequence. Whatever the explanation of the history of cementation, it is difficult to visualize  
409 such structures as having resulted from permineralization of sponge tissues essentially  
410 because the key issue is the problem of recognizing that the structure was originally  
411 sponge tissue.  
412

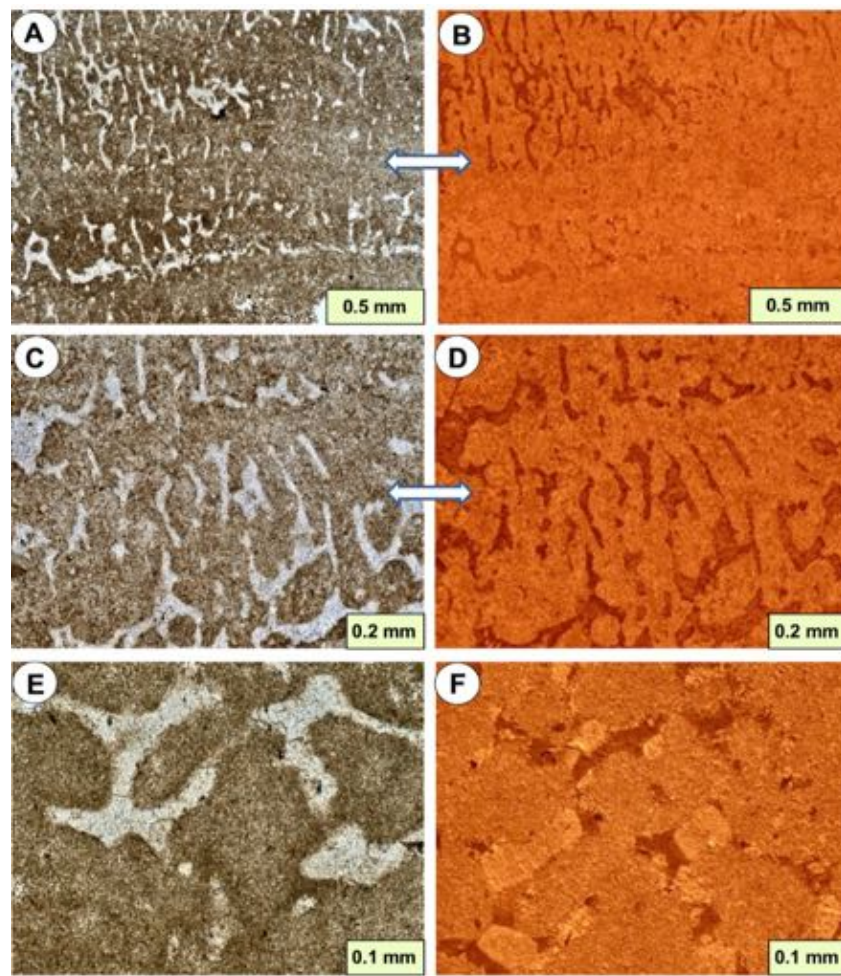


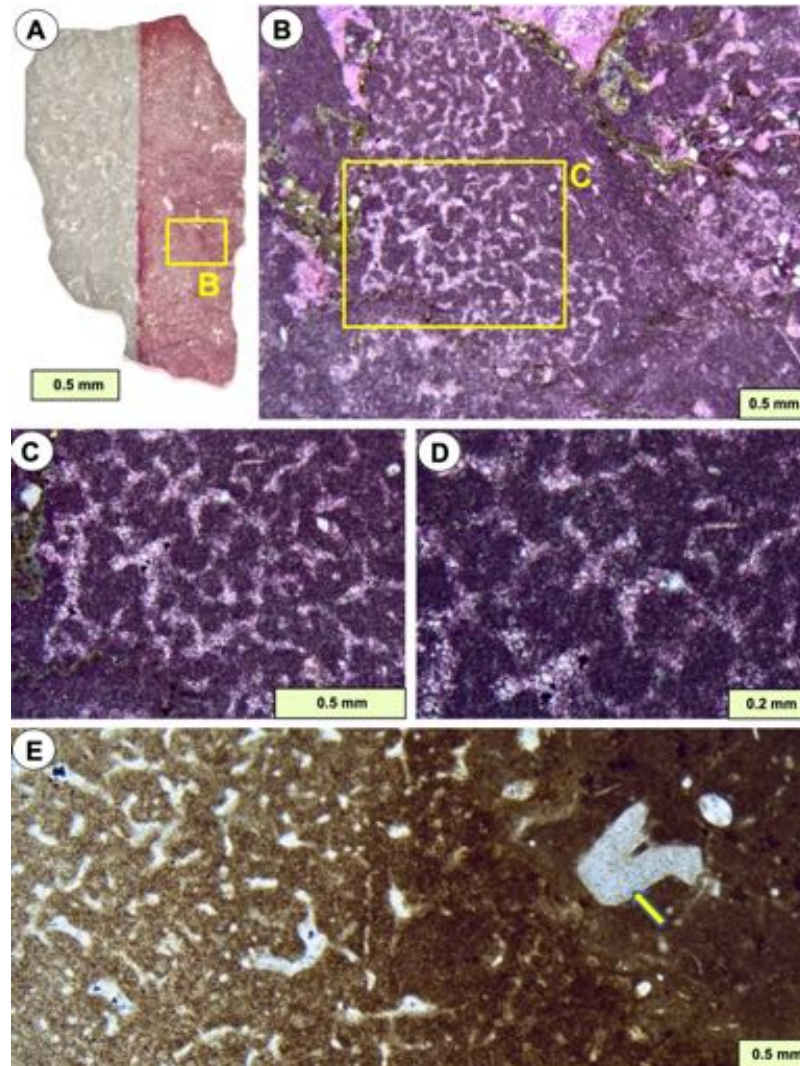
**Figure 8** – Vertical sections from a stromatolitic horizon, containing vermicular structures. (A, B) PPL (A) and CL (B) views of prominent vermicular structure in stromatolite. (C, D) Detail of structure from an adjacent area of thin section to A and B. (E, F) Detail of another area of this sample at greater enlargement. Images in this figure demonstrate the difference in CL response between the sparite and micrite areas, indicating their diagenetic histories are not coincidental. From the collections of Joachim Szulc, sampled by him from the Ladinian (late Middle Triassic), Negev area, Israel.

413  
414  
415  
416  
417  
418  
419  
420  
421  
422  
423  
424  
425  
426  
427  
428  
429  
430  
431  
432  
433  
434  
435  
436  
437  
438  
439

### Network fabrics

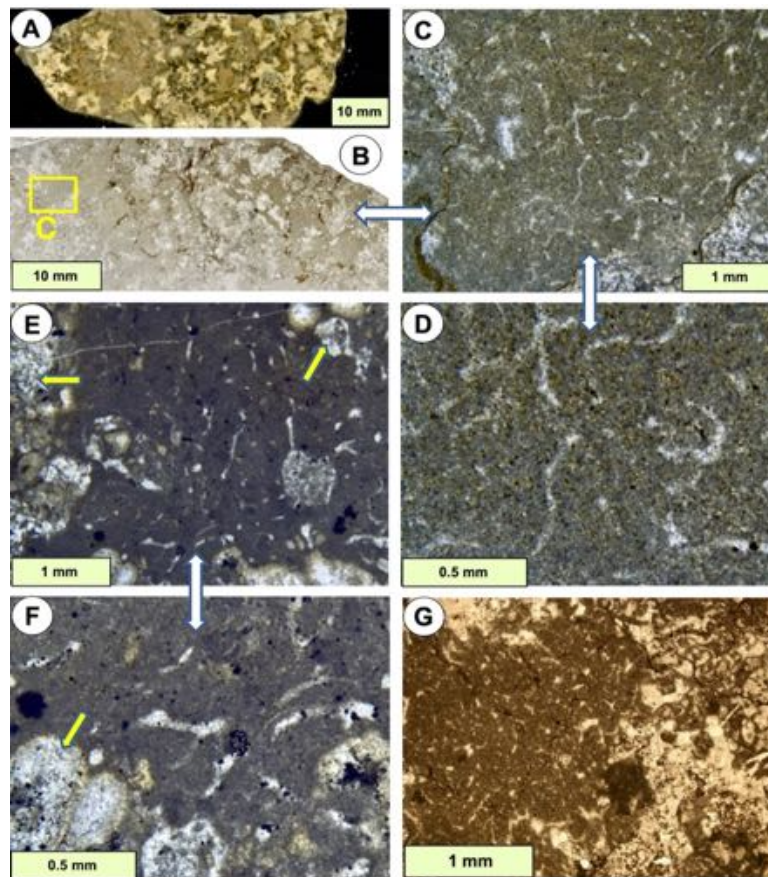
Networks are composed of narrow areas of sparite surrounded by micrite, and appear as two broad types: Rectilinear networks comprising mostly criss-crossing straight lines of sparite with nodes (Figs 3E, F; Fig. 4A-D), that are reasonably interpreted as spiculate sponges; and Curved networks of uncertain origin comprising convoluted curved areas of sparite (Figs 9-12), which vary in structure from those with equal thickness sinusoidal sparite-filled areas to those that are more haphazardly arranged. Both Rectilinear and Curved network types in thin section give the impression that they must exist as a three-dimensional (3D) network (e.g. Luo & Reitner 2014, 3D reconstruction).-Rectilinear and Curved networks in some cases resemble opaline spicule networks known from well-preserved Palaeozoic Heteroscleromorphs (lithistids; Figs 3F, 4 and possibly Fig. 9). Curved networks are illustrated in numerous studies from Neoproterozoic (Fig. 11E, F reproduced from Turner, 2021), Cambrian, Ordovician (e.g. Lee & Hong, 2019) and Permian-Triassic boundary microbialites (Brayard *et al.*, 2011; Friesenbichler *et al.*, 2018; Baud *et al.*, 2021; Wu *et al.*, 2021). Network fabrics found within micrite inside articulated shells, embedded in micritic matrix lacking the nextworks, were interpreted by Park *et al.*, (2017, fig. 3) as spicule networks. Fig. 10 shows examples of curved networks and

440 microbial structures within microbialites directly after the end-Permian extinction; and Figs.  
441 11A-D and 12 explore more variations in Triassic curved networks using both plane light  
442 and cathodoluminescence (CL), showing the variation in diagenetic history between the  
443 sparite areas and micrite areas. In particular, curved networks may grade into peloidal and  
444 amalgamated fabrics described below.  
445  
446  
447



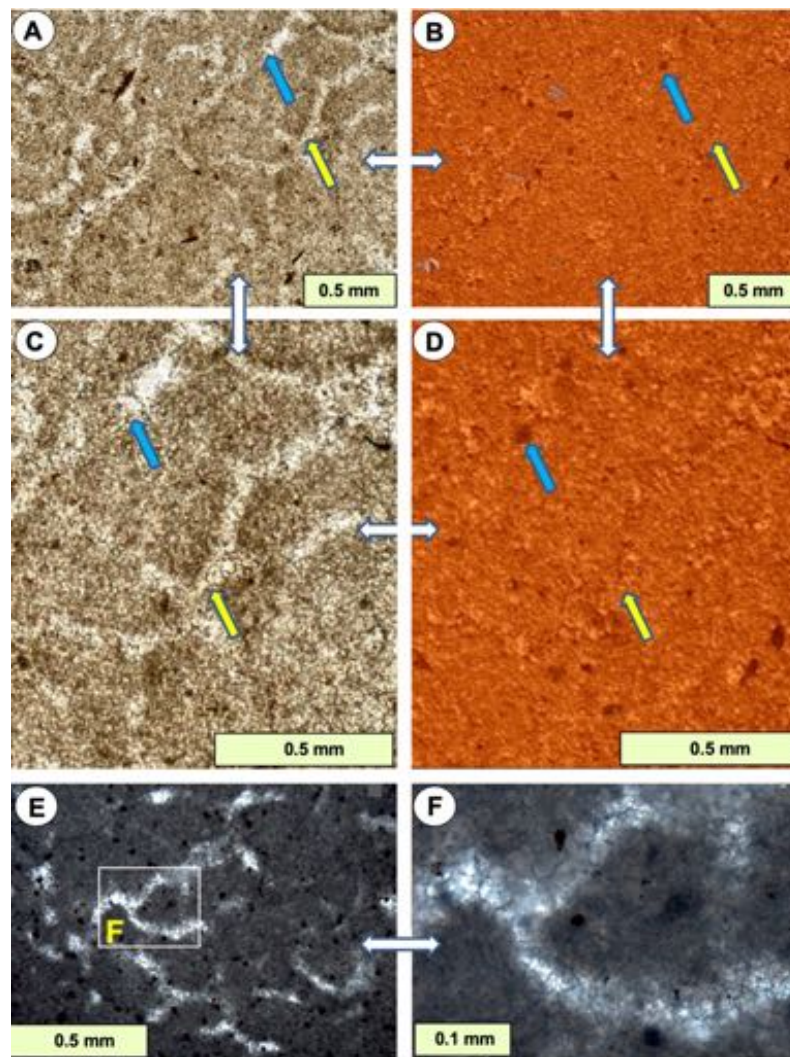
448  
449 **Figure 9** – (A-D) Vertical sections through a small piece of limestone collected from matrix between  
450 stromatolite columns, showing a possible keratose sponge, although this is instead possibly a lithistid. (A)  
451 Whole thin section partly stained with ARS-KFeCN, showing a mottled fabric and the location of B. (B) The  
452 possible sponge forms a defined patch and shows a curved network of sparite-filled voids embedded in  
453 micrite. (C, D) Details of B (D is a detail of centre of C) showing the sparitic nature of the network preserved  
454 as red-stained (non-ferroan) calcite. A-D from Chalk Knolls, Notch Peak Formation, upper Cambrian, Utah.  
455 (E) Curved network of sparite in micrite, but with a diffuse margin; a crinoid columnal (arrow) is prominent in  
456 right hand part, outside the network. The network area may be a sponge, but its diffuse margin presents a  
457 problem of interpretation (Kershaw et al. 2021a). Huashitou reef, Ningqiang Formation, Telychian (lower  
458 Silurian), Guangyuan, northern Sichuan, China; specimen donated by Yue Li.  
459  
460  
461





462  
463 **Figure 10** – Examples of network fabrics in Permian-Triassic boundary microbialites from south China. (A, B)  
464 Hand specimen (A) and thin section (B) of microbialite a few cm above the end-Permian mass extinction  
465 horizon, showing recrystallised microbial calcite (lobate pale areas in B) with intervening micrite. (C, D)  
466 Enlargements of yellow box in B showing curved sparite areas in the micrite, that are of similar material to  
467 that interpreted as keratose sponge by Baud *et al.* (2021) and Wu *et al.* (2021). Permian-Triassic boundary  
468 interval, Baizhuyuan site, Huaying Mountains, Sichuan, China. (E, F) Another sample of microbialite after the  
469 end-Permian extinction, with curved sparite patches as in A-D, but in this case may comprise bioclasts.  
470 These two images also show lobate areas of light-coloured sparite in the edges (arrows), that are the  
471 calcimicrobe frame which constructed the microbialite (Kershaw *et al.*, 2021b). Laolongdong site, Beibei,  
472 Chongqing, China. (G) The right-hand third of this view shows partially altered calcimicrobial structure,  
473 comparable to that described by Ezaki *et al.* (2008, Fig 8C from the Dongwan locality a few km along strike)  
474 as “spongelike”, mistakenly interpreted as sponges by some authors, see text for discussion. The left-hand  
475 two thirds show micrite infill, containing network fabrics, deposited between microbial branches. See text for  
476 discussion. Baizhuyuan site.

477  
478  
479



480  
481  
482  
483  
484  
485  
486  
487  
488  
489  
490  
491  
492  
493  
494  
495

**Figure 11** – (A-D) Vertical sections of vermicular structure in PPL and CL views. (A) light branched and curved areas are sparite embedded in micrite. (B) CL view of the same area as A. (C, D) Enlargements of A and B respectively; arrows show matched points in the four photographs. The CL view (B, D) shows little difference in luminescence pattern between the two components; the sparite contains poorly luminescent and bright luminescent areas, and the micrite shows a similar variation at a smaller scale, in fine grained material, giving it a speckled appearance. Some portions of the sparite are indistinguishable in the CL view.

Whether this arrangement of PPL and CL patterns supports or denies a keratose sponge origin of the vermicular structure is open to discussion. From the boundary between Diplora Beds and overlying Tarnowice Beds, Muschelkalk, Middle Triassic, Libiąż Quarry, Upper Silesia, Poland. (E, F) Vermicular structure from Neoproterozoic carbonates described by Turner (2021, Extended data Figure 1B-C. Note the sparite-filled network fabric. Reproduced under Creative Commons licence (<http://creativecommons.org/licenses/by/4.0/>), with acknowledgment to Nature.

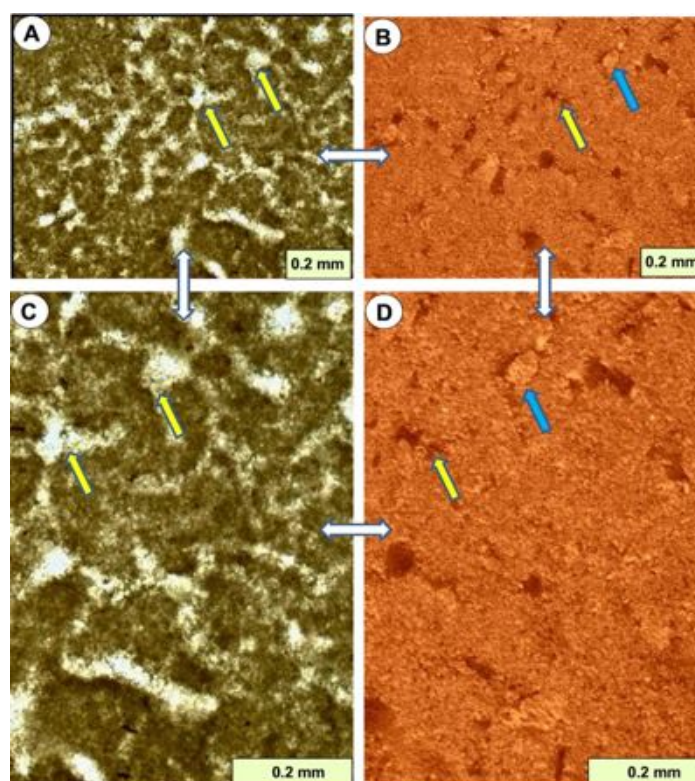


**Figure 12** – Vertical sections of vermicular structure in PPL and CL views, for comparison with Figs 7, 8 & 11. (A) Light branched and curved areas are sparite embedded in micrite; (B) is the matched CL view. (C, D) Enlargements of A and B respectively; arrows show matched points in the four photographs. Although initial examination indicates differences from Figs 7, 8 & 11, CL patterns in these figures only show variable amounts of poor and bright luminescent areas in the sparite, yet some parts of the sparite are also indistinguishable from the micrite in CL view. Collected from the boundary between Diplora Beds and overlying Tarnowice Beds, Muschelkalk, Middle Triassic, Libiąż Quarry, Upper Silesia, Poland.

496  
497  
498  
499  
500  
501  
502  
503  
504  
505  
506

### Amalgamated fabrics

Amalgamated structures comprise patches of micrite, which in some cases give the impression of a vague individuality merged together with intervening spaces occupied by sparite (Fig. 8, which also shows layers, visible in Fig. 8A, B); samples viewed with CL show different cements in the sparite areas compared to the micritic areas, thus indicating voids filled with cement. They overlap with the concept of clotted micrites, but clotting implies a process of sedimentary material sticking together, which may or may not be appropriate in this case, so amalgamated is used here. The possibility exists that some measure of diagenetic change may have affected such material. Amalgamated fabrics have been described as keratose sponges by Lee *et al.* (2014) and Park *et al.* (2017, fig. 3), and were the subject of discussion by Kershaw *et al.* (2021a) in comparison with possible sponges.

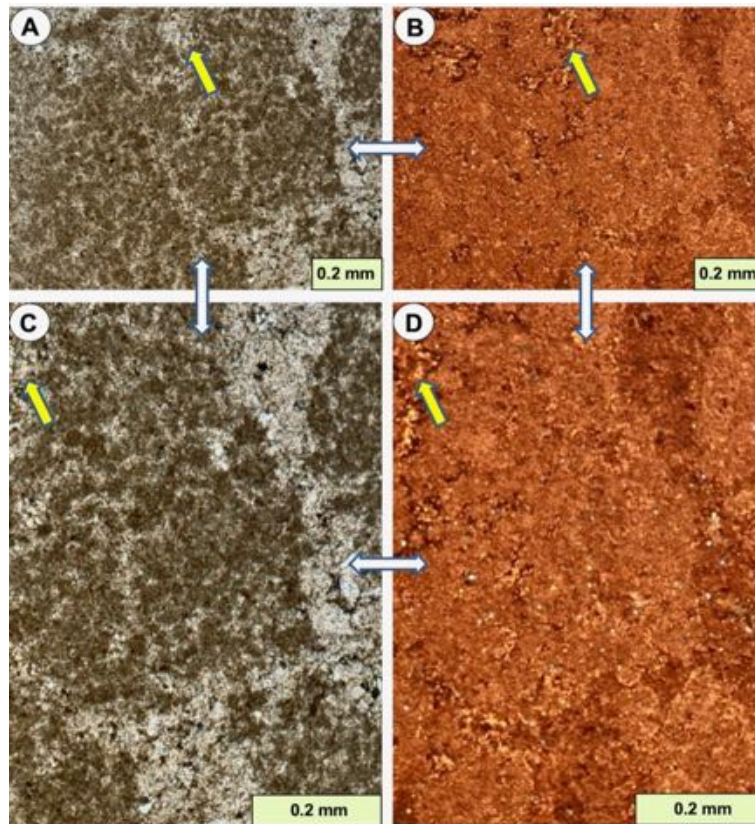
519

### Granular fabrics

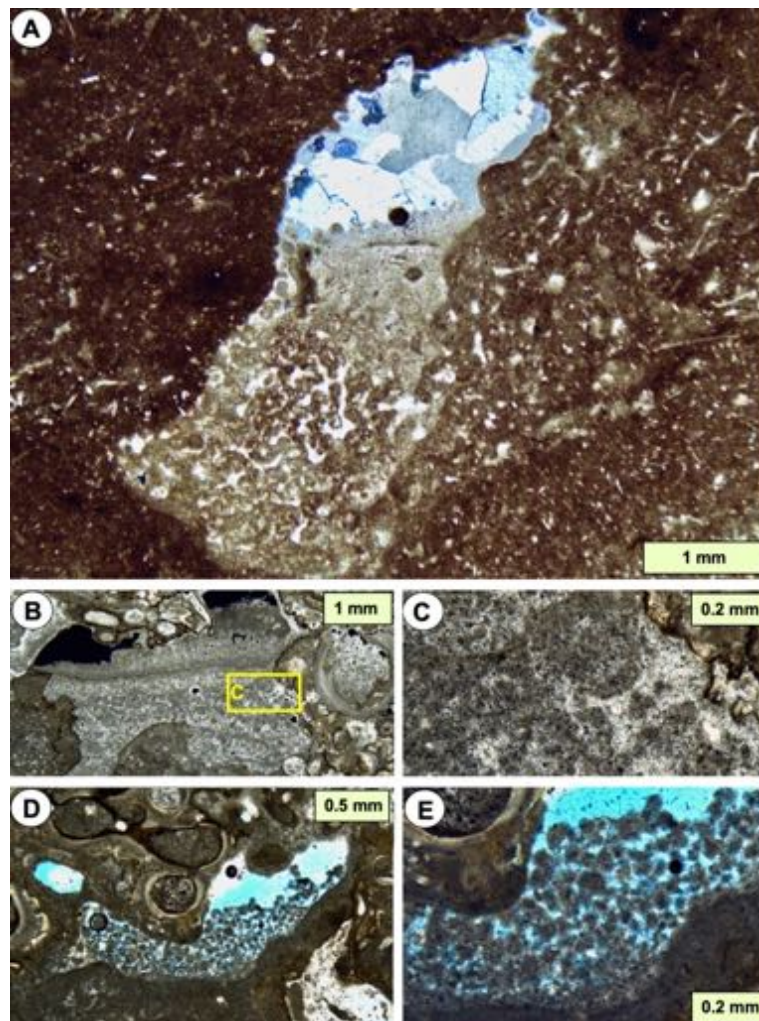
The Granular category comprises micritic objects with irregular areas of sparite cement in spaces between objects (Fig. 13). In their simplest appearance they may be described as peloids and commonly occur in cavities forming geopetals (Fig. 14, but compare with Figs. 16 and 17 considered in the discussion). In many of the cases similar to Fig. 14 attributed by authors to keratose sponges (e.g. Lee & Hong 2019, fig. 2; Park *et al.*, 2017, fig. 3E, F), the granular fabric grades downwards into the amalgamated fabric, that is, these fabrics give the impression of an evolution of fabric from particulate to amalgamated in function of

527

528 stratigraphic polarity and packing density. Because disaggregation of peloids into more  
529 diffuse masses of micrite is a common phenomenon, careful observation of the  
530 intergranular and shelter porosity (thickness variation, grain-supported texture, sagging  
531 and dragging along pore walls) holds the key for discrimination of an essentially physical  
532 (abiotic) origin.  
533



534  
535 **Figure 13** – Vertical sections of pelletoidal structures from Viséan limestones of the Boulonnais inlier, N.  
536 France. (A, B) PPL (A) and CL (B) views of peloidal carbonate, showing bright orange luminescence of  
537 peloids; and dull orange to yellow luminescence of interpeloidal calcite cement. (C, D) Details of the  
538 structure, arrows mark matched points. These images are provided here to demonstrate that peloidal fabrics  
539 are not compatible with the interpretation as sponges, and may instead be particulate carbonate or  
540 microbially deposited; there is no reason to consider these as sponges.  
541  
542



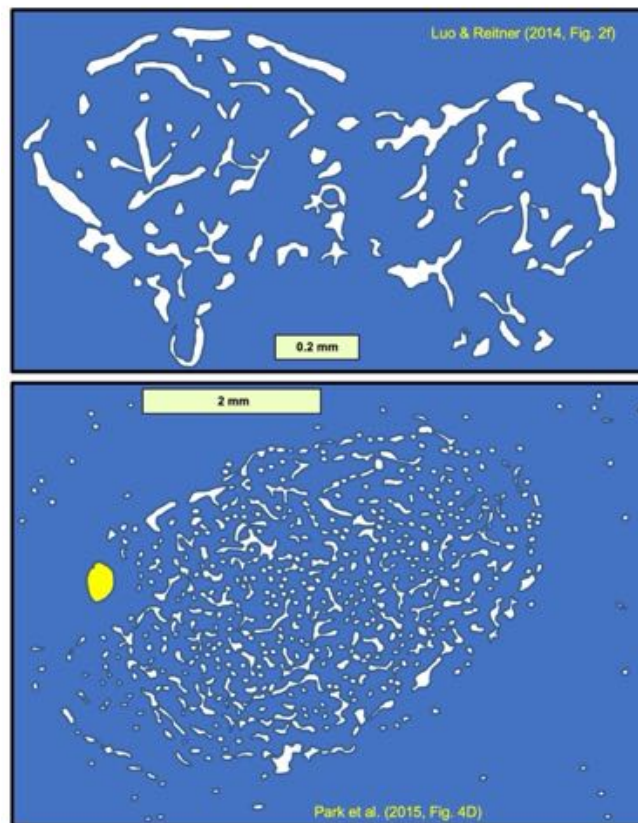
543  
544  
545 **Figure 14** – Vertical sections through geopetal fabrics in early-formed cavities in shallow marine limestones,  
546 containing peloidal and clotted micrites. (A) Geopetal cavity in a mud-rich coral reef, shows variation from  
547 separate peloids at the top down to amalgamated fabrics in the lower part; these were interpreted by  
548 Kershaw *et al.* (2021a) to be either inorganic or microbially related structures, in contrast to the interpretation  
549 of similar structures as keratose sponges. Huashitou reef, Ningqiang Formation, lower Silurian, Guangyuan,  
550 N. Sichuan, China. Reproduced from Kershaw *et al.* (2021a), under CC-BY-NC 4.0, with acknowledgement  
551 to Yue Li, The Sedimentary Record and SEPM. (B, C) Geopetal cavity in an algal reef, with layered peloids  
552 interpreted as sedimentary, with possible microbial influence. Note that B is in XPL and the two black areas  
553 at the top are holes in the thin section; C is in PPL. Late Quaternary, Aci Trezza, eastern Sicily, Italy; after  
554 Kershaw (2000). (D, E) Geopetal cavity in algal-coral reef with interpreted particulate peloids and cements.  
555 Both images are PPL; blue colour is resin-filled empty space in the geopetal. Holocene, Mavra Litharia,  
556 central south coast of Gulf of Corinth, Greece; after Kershaw *et al.* (2005).  
557  
558

### 559 **Variegated spar fabrics**

560 In some cases attributed to keratose sponges, a separate category of sparite within micrite  
561 masses comprises a structure that appears to be organized differently from the Networks  
562 described above (Fig. 15, diagrams traced from publications). Variegated structures  
563 comprise an outer portion of short lines of sparite that curve round to form the outer limits  
564 of a discrete structure, and the inner portion is similar to the Network forms described  
565 above. Examples are in Luo & Reitner (2014, fig. 2f), Park *et al.* (2015, fig. 4D; 2017, fig.  
566 4C) and Friesenbichler *et al.* (2018, fig. 10B). These variegated structures are different  
567 from the curved networks and are presumed to have been formed by a different process;  
568 they seem to occur mostly in cryptic positions, although the case illustrated by  
569 Friesenbichler *et al.* (2018, fig. 10B) is in open space between microbialite branches.

570

571



572

573

574

575

576

577

578

579

580

581

582

583

584

585

586

587

588

589

590

591

592

593

594

595

596

597

598

**Figure 15** – Traced drawings of variegated fabrics, from (A) Luo and Reitner (2014) and (B) Park et al. (2015) to show the pattern of sparite (white), with an outer broken border of curved areas of sparite. The blue background in each case is micrite lacking any clotted or automicrite fabrics and is presumed to be deposited sediment. In B the yellow ellipse is likely an ostracod shell.

## DISCUSSION

The issue expressed in this study is that structures considered to be keratose sponges by numerous authors are unverified, and are even unlikely because of the preservation issues. Thus, such features can be interpreted as other structures, as indicated in the Results section and discussed below. There are four principal areas of concern: 1) verification of the keratose (aspiculate) sponge affinity; 2) alternatives to sponges; 3) accuracy of reporting; and 4) the impact on understanding of ancient ecosystems. One of the prominent difficulties in assessing published illustrations is the low resolution of images, and the common use of thick microscope sections that lack clarity.

### Verification of keratose sponge affinity

The wide variety of fabrics attributed to keratose sponges in the ancient record suffers from lack of verification and coherence, and in the case of the report by Turner (2021) of an early Neoproterozoic example (Fig. 11E,F), the age predates significantly the time corridor predicted for keratose sponges by molecular phylogeny (Fig. 5). In few cases are a mesoscopic body or overall shape reported. Even at the microscopic scale, there is a fundamental problem because no mineralized sponge fabrics are certainly identified, so that preservation of the purported spongin skeleton requires understanding of a diagenetic pathway that seems to have no equivalent in the rock record.

599 Overall, the claim for fossil keratose sponges in ancient carbonates requires both a  
600 proper identification of sponge structure in concert with an exceptional preservation  
601 mechanism. Indeed, relatively decay-resistant structural tissue components such as parts  
602 of the extracellular collagenous matrix (ECM), mesoscopic strands and networks of  
603 spongin, the various forms of chitin ( $\alpha$ ,  $\beta$ ,  $\gamma$ ) and cellulose might get physically preserved  
604 or replicated *via* permineralisation or *via* polymerisation (Gupta & Briggs, 2011). For the  
605 claim of keratose sponges in carbonates, permineralisation (mummy-style preservation) of  
606 the sponge to produce automicrite is considered a prerequisite in order to eventually  
607 preserve in 3D a former network of spongin as a calcite-cemented mold. Otherwise, if only  
608 the spongin was polymineralised (or permineralised) the result should be severe physical  
609 compaction only episodically preserving exceptional details (Burgess-style preservation of  
610 sponges; Conway Morris & Whittington, 1985; Butterfield & Nicholas, 1996).

611  
612 *Sponge mummies, indirect replication of a former spongin skeleton*

613 For a keratose sponge to permineralise it would be necessary to replace the sponge tissue  
614 with micrite. Froget (1976, on lithistids) followed by Brachert *et al.* (1987, on hexactinellids)  
615 provided examples of Pleistocene to Holocene permineralised (calcified) siliceous  
616 sponges. In addition, these authors observed in some detail the concurrent onset of  
617 diagenetic alteration of the opaline spicules (dissolution, recrystallisation to calcium  
618 carbonate, initial cementation). Reitner (1993, p. 26 and Pl. 4/4) illustrated how a living  
619 non-rigid demosponge might preserve its original spicular architecture within automicrite.  
620 Neuweiler *et al.* (2007) interpreted an intimate connection of mummification with calcifying  
621 organic colloids adsorbed onto and into relatively decay-resistant parts of the former ECM,  
622 thus dismantling fibrillar collagen during partial death. However, because spongin is a non-  
623 fibrillar collagen (Exposito *et al.*, 1991), during decay, no dismantling into submicroscopic  
624 collagen fibers with their associated secondary sorptive attributes (surface area,  
625 scaffolding; Neuweiler *et al.*, 2007) is expected to occur. Indeed, permineralising  
626 (petrifying) modern sponges, except for being a curiosity, typically are very rich in fibrillar  
627 collagen giving them a firm-leathery (e.g. the spiculate *Sphaciospongia*, Wiedenmayer  
628 1978) to even cartilaginous consistency (e.g. the petrifying verongimorph *Chondrosia*,  
629 Göthel, 1992). Nevertheless, it remains questionable whether that small group of extant  
630 sponges is representative of fossil sponge mummies (Neuweiler *et al.*, 2007 for full  
631 discussion). In many sponges, there is a problem of sheer volume, that is the amount of  
632 ECM present in a modern sponge does not match the larger amount of automicrite present  
633 in sponge mummies (see *Malumispongium* in Bourque & Gignac, 1983; Neuweiler *et al.*,  
634 2007), therefore unresolved microbial-organochemical reactions might be involved, and  
635 even dissolved pore-water silica might play a role if opaline spicules were originally  
636 abundant (Lakshatanov & Stipp, 2010). Thus if the sparite portions of a vermicular structure  
637 represent the spongin of a keratose sponge, then transformation from spongin to sparitic  
638 calcite (with perhaps an intermediate step not preserved) would have to occur **after**  
639 conversion of the intervening soft tissue to micrite to prevent compression of the spongin  
640 network in burial.

641 It should be noted here that the spar-micrite structures illustrated in Luo & Reitner  
642 (2014, 2016), Lee & Riding (2021a, b) and Turner (2021), in concert with our own results,  
643 do not show major compression. Automicrite (mummification) is stated as being present,  
644 but no supporting petrographic or geochemical evidence is provided (parameters include:  
645 gravity-defying, secondary porosity, fragmentation, local collapse, fluorescence,  
646 intracrystalline organic compounds; Neuweiler *et al.*, 2000). Another example of the  
647 problem of verification is shown in Heindel *et al.* (2018, Figs. 9D, 10B, D), who illustrated  
648 microbialites from the well-known Çürük Dag site in southern Turkey. Heindel *et al.*  
649 labelled sponges as being present in the matrix that sits between microbial branches, but

650 close examination of those images reveals a calcareous mudstone with minute bioclasts  
651 and cannot be considered a sponge mummy. Other images in the same paper show areas  
652 of matrix containing fine sparite between microbial branches that may be networks, but  
653 there is no demonstration of criteria to indicate that these are sponges mummies; a similar  
654 example from south China was discussed by Kershaw *et al.* (2021a).  
655

#### 656 *Discrete replication of a spongin skeleton*

657 It is conceivable that the spongin itself might be replicated via polymineralization or  
658 permineralization, but then preservation of an organic phase (plus compression) or ghost-  
659 structures within a permineralizing phase would be expected (Gupta & Briggs, 2011). As  
660 noted above, in opposition to the fibrillar collagen in sponge ECM, spongin is a non-fibrillar  
661 collagen (Exposito *et al.*, 1991) and during decay or partial death, no dismantling or  
662 enhanced secondary sorptive attributes supporting permineralisation (Neuweiler *et al.*,  
663 2007) are envisaged. Another option is coating, that is mineral precipitation and growth at  
664 and from the spongin surface (see Szatkowski *et al.*, 2018), but no respective fabric  
665 relationship has been reported. The CL images presented in Figs. 7, 8, 11-13 largely show  
666 the sparite portions to have different cements from the micrite; in some cases (e.g. Fig. 7F,  
667 8, 12) there are zoned cements in the sparite that indicate early porosity and permeability,  
668 so this seems to preclude any mineralization process related to the spongin itself, at least  
669 for these samples. Even in Fig. 11A-D, where the distinction between the micrite and  
670 sparite areas in CL is minimal, parts of the sparite show different CL response from the  
671 micrite. Thus, in the cases illustrated in this paper, there is no obvious basis for  
672 mineralization of the spongin itself to explain the sparitic areas. It is easier to explain the  
673 CL images in terms of various kinds of early and fabric-selective porosity. Nevertheless,  
674 this does not necessarily deny a sponge affinity but leaves mummification as the only  
675 option left to explain preservation of keratose sponges in carbonate rocks. However, as  
676 stated earlier, the petrographic or geochemical evidence for mummification is either  
677 unclear or absent. Finally, there are sponges which contain opaline spicules attached to  
678 prominent strands of spongin (Axinellidae) which as fossils should show both spicules  
679 together with their associated replication of spongin. No published report of such an  
680 intimate relationship preserved in carbonate rock thin-sections was found in the literature.  
681

#### 682 *Other issues*

683 A significant aspect of observation in relation to sponge affinity in thin-section relates to the  
684 pore- and canal system specific to sponges (Figs 1A, B; 2C, D). If sponge mummies are  
685 present, a canal system might be preserved in astonishing detail (Neuweiler *et al.*, 2007;  
686 2009) even in the absence of a spicular skeleton (Bourque and Gignac, 1983; Neuweiler *et al.*  
687 *et al.*, 2007, their Fig. 1 A, B). Indeed, Aragonés & Leys (2022) proposed a model for fossil  
688 sponge recognition based on the presence of a canal system. However, there are no  
689 respective features in all the fossil examples illustrated here and in publications examined  
690 in this study. Neuweiler *et al.* (2009) denied the presence of sponges in early  
691 Neoproterozoic polymuds because of the lack of any signs of a preserved canal system.  
692 On the other hand, the canal system (together with spicules) might be too tiny to be  
693 visually replicated, although other observations (automicrite, context, substrate) may  
694 indicate a sponge interpretation (Shen & Neuweiler, 2018). Lee & Riding's (2020)  
695 reconsideration of the enigmatic structure *Cryptozoön* provides an excellent example of  
696 the overall problem of sponge recognition. The fabric interpreted as keratose sponge in  
697 Lee & Riding's (2020, fig. 5c, d) looks somewhat different from the supposed keratose  
698 standard image in their fig. 9c, but instead resembles, but not fully matches, the lithistid in  
699 their fig. 9a. Despite high quality preservation, there is no (hierarchical) canal system,



700 there is no cortical architecture and there is no analysis of diagenesis. Evidence for the  
701 presence of keratose sponges (in opposition to conventional (microbial) spongiostromata)  
702 is needed to test the original interpretation (Luo & Reitner 2014, 2016).

703 In summary (see also Table S1), without verification the presence of fossil keratose  
704 sponges in thin-sections made from limestones-dolostones is called into question. Table  
705 S1 represents an effort to requalify the most prominent examples as: essentially microbial  
706 (spongiostromate, birdseyes-vugular-fenestral porosity), biogenic-problematic, and dubio-  
707 to even pseudofossil in nature.

708

## 709 **Alternatives to sponges**

### 710 *Endobenthos*

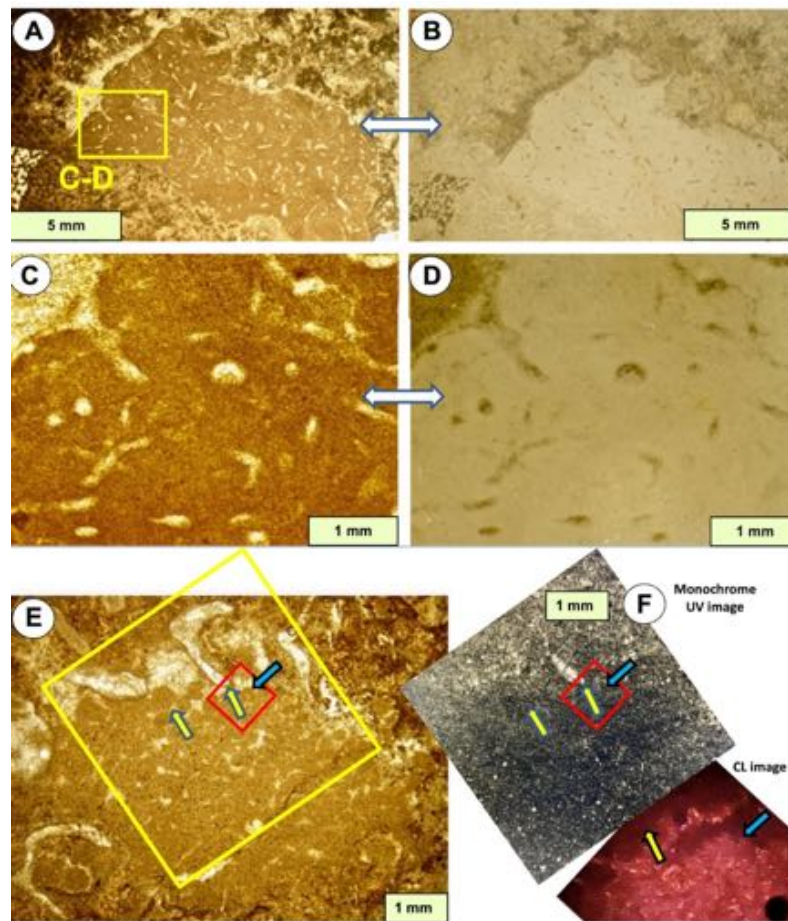
711 Geopetal cavities in lithified limestone and in articulated shells show a common pattern  
712 where the upper part of the deposit comprises peloids, that grade downwards into  
713 amalgamated micrite within the cavity, as noted earlier (e.g., Fig. 14). Several of these  
714 examples are reported as sponges (Lee & Hong, 2019, fig. 2) but they are easily  
715 recognizable as peloidal micrites that merged downwards to form clotted structures. The  
716 formation process of such features is not obvious. Although they may be considered as  
717 reflecting compaction in the sediment mass, it is notable that compaction requires  
718 sufficient mass of material to enable gravitational compression, which seems unlikely in  
719 such small structures. An alternative is that they may reflect small-organism activity in the  
720 cavities, and thus could be meiofauna. The concept of meiofauna (organisms of sizes  
721 between micro- and macro-fauna, up to 1 mm size) is well-developed in biological  
722 literature (Semprucci & Sandulli, 2020) but almost unknown in the ancient record (e.g.  
723 Knaust, 2010). The ability of meiofaunas in modern environments to create burrows and  
724 microborings provides a viable alternative to at least some of the possible keratose sponge  
725 interpretations described in this study.

726 Micro-organismic activity is proposed to explain some carbonate facies  
727 (McMenamin, 2016), with common occurrence in protected locations such as cavities and  
728 empty shells lying on the ancient seabed. Fig. 16 shows a Cambrian example of potential  
729 microboring networks in a cavity, noting that the images also indicate geopetal sediment in  
730 the sparite areas indicating an open network prior to cementation. Fig. 16E, F explores the  
731 use of UV fluorescence microscopy and shows in this monochrome image that the brighter  
732 areas (therefore presumably containing more organic matter) are outside the area of the  
733 network; this is interpreted to indicate that the network was not composed of automicrite  
734 and thus not related to sponge degradation. The accompanying CL image (Fig. 16F)  
735 indicates brighter luminescence in the sediment that may reflect diagenetic alteration. Fig.  
736 17 shows a case of cavities inside the outer portion of a stromatolitic dome in shallow  
737 marine platform carbonates from North China; the cavities contain micrite and some type  
738 of network that does not resemble a sponge, and may be interpreted as a microboring net.  
739 In the view of the authors of this study, the examples of peloidal and network structures  
740 found in cavities and shells cited above are open to be reinterpreted as meiofauna  
741 (microscopic faunas) rather than sponges.

742

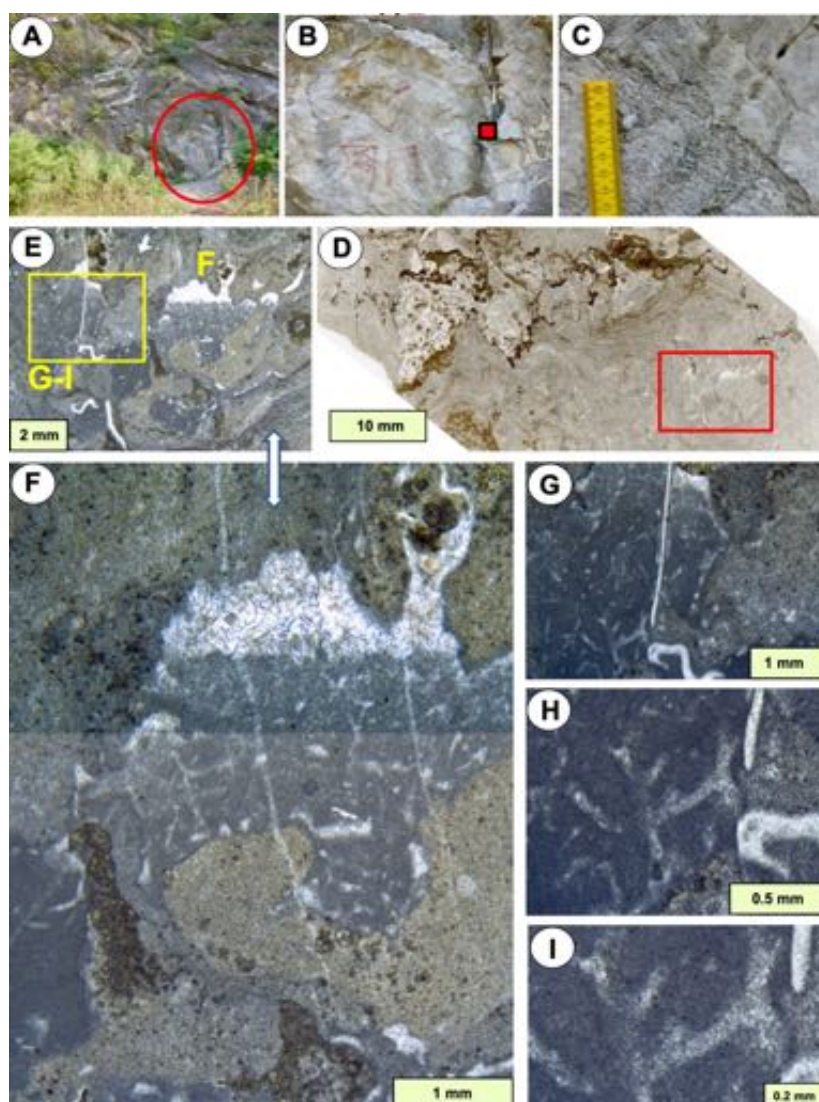
743

744



745  
746  
747  
748  
749  
750  
751  
752  
753  
754  
755  
756  
757  
758  
759  
760  
761  
762

**Figure 16** – Vertical sections through vermicular structures in cavities in Cambrian carbonates, interpreted by McMenamin (2016) as due to the actions of meiofauna rather than evidence of sponges. (A, B) PPL (A) and reflected light (B) views of vermicular structures within a cavity in an archaocyath-algal boundstone. In this example, the vermicular structures are interpreted as possible graphoglyptid trace fossils comprising microburrow swarms, described by McMenamin (2016). (C, D) Details of box in A, using PPL (C) and reflected light (D) views. Puerto Blanco Formation, Lower Cambrian, base of unit 3, Cerro Rajón, Sonora, México. (E, F) Vermicular structure in the interior space of a dead archaocyath, here interpreted as comprising packed faecal pellets in a cavity. E is PPL, F shows UV (upper image) and CL (lower image); red box in the UV image shows location of the CL photo; yellow and blue arrows show matched points between these three images. Pellets are discrete in the upper part of the cavity but become more diffuse downwards, interpreted by McMenamin (2016) to indicate pellets disaggregated in the lower part of the pile and the light areas are interpreted as microburrows in the sediment, the burrowing activity may have caused disaggregation of the pellets. Poleta Formation, Cambrian Stage 3, Barrel Springs, Nevada, after McMenamin (2016).



763  
764 **Figure 17** – Vertical sections through vermicular structures in a cavity within a stromatolite. (A-C) Field views  
765 of a stromatolite bioherm; red box in B shows location of sample, from the upper part of the bioherm; C  
766 shows field detail of stromatolite columns overlain by bedded limestone. (D) Whole thin section view of  
767 stromatolite, showing abundant cavities in its structure, shown clearly in E (red box). (E) Cavities (darker  
768 grey with geopetals) in stromatolite mass. (F) Detail of right side of E, showing vermicular structure in the  
769 geopetal fill. (G-I) Details of left side of E (yellow box) showing branched structure of light areas of sparite  
770 within the micrite fill of the cavity. These are interpreted here as possible microburrow networks of  
771 meiofauna, and not of sponges. Uppermost Gushan Formation, upper Cambrian, Xiaweidian, near Beijing,  
772 China.  
773  
774

775 Verification of evidence of ancient meiofauna in sedimentary rocks is in early  
776 development (Dirk Knaust, Pers. Comm. 2021; see also McIlroy, 2022). Meiobenthic trace  
777 fossils are a relatively new field of ichnology. In the small number of available publications  
778 (e.g. Knaust, 2007), foraminifers, nematodes, annelids (particularly polychaetes),  
779 arthropods (ostracodes, malacostracans) are listed as the most plausible producers,  
780 sometimes being preserved at the end of the trace (Knaust, 2007). Meiofauna burrows  
781 may be identified by their constant diameter and regular winding to sinusoidal character,  
782 features that are seen in some published photos interpreted by some authors as keratose  
783 sponges (e.g., Park *et al.*, 2015, fig. 8A), and may explain the fabrics reproduced here in  
784 diagram form in Fig. 15). Knaust (2007) felt confident to name some cases as trace fossil  
785 ichnotaxa, e.g. *Cochlichnus* Hitchcock 1858. Meiofauna burrows are expected to  
786 concentrate in organic-rich areas of the sediment, such as within macrofauna burrows or

787 whole shells; in this context the features in Luo & Reitner (2014, fig. 2f) and Park *et al.*  
788 (2015, fig. 4D), reproduced in Fig. 15, are potential macrofaunal burrows penetrated by  
789 meiofauna, whereas the figure Park *et al.* (2015, fig. 8B) presents a whole brachiopod  
790 shell that may have been passively filled with micrite and subsequently penetrated by  
791 meiofauna to produce vermicular-structured micrite.

792

### 793 *Dubio- to Pseudofossils*

794 3D spar-micrite micro-networks might result from cementation of interparticle porosity of  
795 fine-grained granular-pelletoidal sediment material, an important source of ambiguity of  
796 carbonate rock petrography (Macintyre, 1985; Lokier & Al Juanabi, 2016; Kershaw *et al.*,  
797 2021a). The issue is complicated because the initial state and cohesiveness of peloidal  
798 material varies greatly from loose aggregates-floccules to indurated grains via an entire  
799 spectrum of plasticity (Schieber *et al.*, 2013). The consequences might be severe because  
800 during consolidation and physical compaction the initial granular texture might be lost,  
801 resulting in a grumelous ghost structure or even a diagenetic mudstone texture (Lokier &  
802 Al Juanabi, 2016 for full discussion). Peloidal textures might also result from authigenesis  
803 (automicrite) and heterogenous aggrading neomorphism (Bathurst, 1975; Dickson, 1978;  
804 Macintyre, 1985). The examples of peloidal textures in geopetal infills in cavities presented  
805 by Lee & Hong (2019) as sponges can be alternatively interpreted as peloidal fills in  
806 cavities. In another example, the microspar groundmass in Turner's (2021) study of  
807 Neoproterozoic vermiform structure contains no features that would indicate it originated  
808 through 'permineralization of a pre-existing biological substance' (automicrite). The  
809 illustration of a vermiform microstructure in a shelter void (Turner 2021, extended data, fig.  
810 2) grades into the underlying and overlying homogenous microspar; the lack of a sharp  
811 contact between the vermiform area and adjacent micrite reduces confidence that this  
812 structure is a sponge. The Early Neoproterozoic vermiform microstructure (Turner, 2021)  
813 may indeed be a dubiofossil or even pseudofossil, possibly caused by fluid escape during  
814 the consolidation of a flocculated gel-like carbonate mud (syneresis). Fluid escape, volume  
815 loss and microfolding (Turner 2021, extended data, fig. 2) raises the possibility of  
816 relationship with molar tooth structures of the Neoproterozoic (carbonate gels of Hofmann,  
817 1985 for the Little Dal Group; Kuang, 2014 for review). Furthermore, although they have  
818 some resemblance to microburrow nests observed in Phanerozoic limestones  
819 (graphoglyptid trace fossils, see Kris & McMenamin, 2021), it seems unlikely that  
820 endofaunal metazoans would have existed in the Early Neoproterozoic, so the respective  
821 claim for presence of a worm-like (bilateralian) organism (Kris & McMenamin, 2021) would  
822 even intensify the conflict with respect to molecular-clock divergence-time estimates.

823

### 824 **Accuracy of reporting**

825 As stated earlier, examination of literature on keratose sponges in ancient carbonates  
826 reveals two common features: 1) that all studies refer back to the original 3D  
827 reconstruction study by Luo & Reitner (2014); and 2) that in almost all cases, subsequent  
828 authors regarded these structures as actual sponges without further investigation. Also,  
829 there are cases of misreporting earlier studies, giving the impression of occurrence of  
830 sponges in other sequences, that were **not** stated in the cited works; this has resulted in  
831 cases of inaccurate reporting of possible sponges, without verifying the original sources. A  
832 good example of misreporting may be found in literature on the Permian-Triassic boundary  
833 microbialite (PTBM) sequences. Ezaki *et al.* (2008, fig. 8C) illustrated a fabric they  
834 described as a "Highly amalgamated and interconnected areas exhibiting spongelike  
835 texture with infilling of peloids". This paper was cited by Friesenbichler *et al.* (2018, p. 654)  
836 as an example of sponges in the PTBMs, and subsequently included in the compilation by  
837 Lee & Riding (2021a, table 1) as keratose sponges. However, careful examination of the

838 material illustrated by Ezaki *et al.* (2008, fig. 8) shows that all four images in that figure are  
839 actually partially altered portions of the lobate microbialite constructor of post-extinction  
840 microbialites in South China, now named as *Calcilobes wangshenghaii* (partly illustrated in  
841 Fig. 10G; also see Kershaw *et al.*, 2021b), thus not a sponge. Another example may be  
842 found in Heindel *et al.* (2018) who described “possible keratose sponges”, but these were  
843 referred to as “keratose sponges” in Lee & Riding (2021a, table 1). Examination of  
844 illustrations by Heindel *et al.* (2018), noted earlier, shows that some of those illustrated are  
845 simply carbonate mudstones-wackestones. Thus, the notion of a “sponge takeover” after  
846 the end-Permian extinction, envisioned by Baud *et al.* (2021), which uses the work of  
847 Ezaki *et al.* (2008), Foster *et al.* (2019) and Friesenbichler *et al.* (2018) as examples of  
848 sponges in the microbialite, may be premature.

### 850 **Implications: the four settings**

851 In the introduction section, four settings of interpreted keratose sponges were presented,  
852 and broader aspects of each are stated below to provide perspective of the implications of  
853 this study.

- 854 1. Neoproterozoic possible keratose sponges were proposed by Turner (2021),  
855 therefore indicating possible metazoans at 890 Ma, significantly earlier than the first  
856 appearance of possible metazoans in late Ediacaran Period (ca. 575 Ma, see  
857 Wood, 2016). Turner’s proposal is therefore potentially highly significant, but relies  
858 on verification.
- 859 2. Although the concept of consortia between keratose sponges and microbial  
860 structures is proposed (Lee & Riding, 2021a; Pei *et al.*, 2021a, b), there are no  
861 modern records of keratose sponges as consortia with other organisms in normal  
862 marine environments. Nevertheless, Ellison *et al.* (1996) demonstrated an unusual  
863 mutualism between sponges and roots of mangroves in shallow subtidal  
864 oligotrophic settings in Belize, serving as a reminder of the enormous ability of  
865 sponges. Furthermore, it is important to recognize that sponges have copious  
866 assemblages of bacteria in their tissues, so it does not preclude the possibility of  
867 consortia in ancient times, but the lack of reported consortia between sponges and  
868 stromatolites in modern environments thus means that no modern analogues for the  
869 ancient carbonates have yet been found.
- 870 3. Cambro-Ordovician occurrences of potential keratose sponges reported in  
871 numerous studies have importance for Palaeozoic evolution of the biosphere with  
872 impact on understanding the Great Ordovician Biodiversity Event, noted by Servais  
873 *et al.* (2021) to consist of an episode of change rather than a short-term event. If  
874 sponges occurred in larger abundance than has been recorded by verified sponges,  
875 then there is an important potential impact on the nature of ancient benthic  
876 assemblages across this period. Thus, it is critical to correctly identify the affinity of  
877 these structures before applying them in a wider context of biodiversity.
- 878 4. Related to point 3, rapid and immense shifts in ecosystems after the end-Permian  
879 extinction include a short period of development of microbialites in shallow marine  
880 carbonate settings, the appearance and disappearance of which have not been  
881 explained. However, recent contributions to literature of interpreted presence of  
882 keratose sponges has a significant impact on models of biotic and environmental  
883 change, so correct identification is critical. The Permian-Triassic boundary  
884 microbialites are likely unique in the rock record (Kershaw *et al.*, 2021b), so the  
885 notion of a concurrent sponge increase is enormously potentially influential in  
886 ecosystem analysis. Furthermore, interpretation of keratose sponge expansion after  
887 the end-Permian mass extinction is an attractive idea, corresponding with the notion  
888 of sponge development during the low-oxygen conditions associated with that

889 extinction, because sponges are known to tolerate low oxygen conditions.  
890 Nevertheless, the lack of sponges in modern stromatolites, and lack of verification  
891 of sponges in post-extinction facies means that it is not wise to include sponges in  
892 models. The corollary is that the unverified reports of sponge presence also lead to  
893 uncertainty in the nature of biotic assemblages. In a modern context, there is  
894 increase in sponges in modern coral reef systems that may be a reflection in the  
895 decline of corals, while sponges are more resilient to change. Sponge expansion  
896 after mass extinction is thus an area of great potential interest in understanding  
897 modern changes but needs to be verified. A key point in this debate is that modern  
898 living sponges normally disintegrate and disappear from the biota (Debrenne, 1999)  
899 in a very short period after death, so from the point of view of 'the present is the key  
900 to the past', there is a problem of determining abundance and diversity of sponges  
901 through their geological history, due to poor overall preservation potential.

902 In summary, none of the reported examples of keratose sponges in ancient limestones are  
903 supported by criteria, and in some cases, sponges are demonstrably absent. This does not  
904 necessarily mean that none of the others are keratose sponges, but the lack of proven  
905 sponges now requires a concerted effort of objective science to sort out this problem and  
906 prevent this snowball of uncertainty continuing to grow.

## 907 908 **CONCLUSIONS**

909 Key points emerging from this study are:

- 910 1. The interpretation of keratose sponges (that consist of skeletons lacking mineral  
911 components) in carbonate facies through the Neoproterozoic to Triassic record (and  
912 likely the entire geological record) may or may not be real, with implications for the  
913 palaeobiology and evolution of sponges, and palaeoecology of fossil assemblages.  
914 The interpretation is considered here to be at best unsafe, and at worst incorrect, so  
915 the importance of keratose sponges in geological history remains uncertain.
- 916 2. The problem of how a keratose sponge spongin network may come to be preserved as  
917 sparitic calcite is a critical and unexplained component of diagenesis that needs to be  
918 addressed.
- 919 3. All published studies claiming keratose sponges need to be re-examined to confirm or  
920 deny their presence; such work may overturn current ideas of the role of keratose  
921 sponges.

## 922 923 924 **ACKNOWLEDGEMENTS**

925 During development of this study we are very grateful for discussions with Andrej Pisera,  
926 who made valuable comments on an earlier version of the manuscript, and provided  
927 images used in Fig. 3E,F. Comments from Joe Botting, Marcelo Carrera, Cristina Diaz,  
928 Dirk Erpenbeck, Jongsung Hong, Dirk Knaust, Jino Park, Christine Schönberg, Elizabeth  
929 Turner, Max Wisshak and Gert Wörheide have provided much insight into this study. SK  
930 thanks: Haizhou Wang (China University of Petroleum) for access to Cambrian carbonates  
931 in North China illustrated in Fig. 17; Yue Li (Nanjing Institute) for access to Silurian  
932 carbonates in South China, including images shown in Figs 9 & 14; and Robert Riding  
933 (Tennessee) for access to Cambro-Ordovician carbonates in Utah illustrated in Figs 4 & 9.  
934 CS also thanks: Lucie Goodayle, Natural History Museum, London, Science Photographer  
935 for *Vauxia* images; Tom White and Javier Ignacio Sánchez Almazán, from Natural History  
936 Museum, London, and National Museum of Natural Sciences, Madrid, respectively, for  
937 access to Recent sponges. We gratefully acknowledge information on microborings  
938 provided by Klaudiusz Salamon, who sadly died in early 2022.

939

940

941 **CONFLICT OF INTEREST**

942 There are no conflicts of interest.

943

944 **DATA AVAILABILITY STATEMENT**

945 Not applicable

946

947 **REFERENCES**

948 **Antcliffe, J.B., Callow, R.H.T. and Brasier, M.D.** (2014) Giving the early fossil record of  
949 sponges a squeeze. *Biological Reviews*, **89**, 972-1004.

950 **Aragonés, P. and Leys, S.** (2022) The sponge pump as a morphological character in the  
951 fossil record. *Paleobiology*, DOI: 10.1017/pab.2021.43, pp. 1-16.

952 **Awramik, S.M. and Grey, K.** (2005) Stromatolites: biogenicity, biosignatures, and  
953 bioconfusion. In: *Astrobiology and Planetary Missions* (Eds R.B. Hoover, G.V. Levin, A.Y.  
954 Rozanov and G.R. Gladstone), Proceedings of SPIE, The international society for optics  
955 and photonics, 5906, 59060P1–59060, p.9.

956 **Ax, P.** (1996) *Multicellular animals: A new approach to the phylogenetic order in nature*,  
957 Volume 1: New York, Springer, 225 p.

958 **Bathurst, R.G.C.** (1976) Carbonate Sediments and their Diagenesis. *Developments in*  
959 *Sedimentology*, **12**, 658 p. Elsevier.

960 **Bathurst, R.G.C.** (1982) Genesis of stromatolite cavities between submarine crusts in  
961 Palaeozoic carbonate mud buildups. *Journal of the Geological Society*, **139**, 165–181. doi:  
962 DOI.org/10.1144/gsjgs.139.2.0165.

963 **Baud, A., Richoz, S., Brandner, R., Krystyn, L., Heindel, K., Mohtat, T., Mohtat-Aghai, P.**  
964 **and Horacek, M.** (2021) Sponge Takeover from End-Permian Mass Extinction to Early  
965 Induan Time: Records in Central Iran Microbial Buildups. *Frontiers in Earth Science*, **9**,  
966 586210.

967 **Botting, J.P., Muir, L.A., Zhang, Y., Ma, X., Ma, J., Wang, L., Zhang, K., Song, Y. and**  
968 **Fang, X.** (2017) Flourishing sponge-based ecosystems after the end-Ordovician mass  
969 extinction. *Current Biology*, **27**, 556-562.

970 **Bourque, P.-A. and Boulvain, F.** (1993) A Model for the Origin and Petrogenesis of the Red  
971 Stromatolite Limestone of Paleozoic Carbonate Mounds. *Journal of Sedimentary*  
972 *Research*, **63**, 607-619.

973 **Bourque, P.-A. and Gignac, H.** (1983) Sponge-constructed stromatolite mud mounds,  
974 Silurian of Gaspé, Québec. *Journal of Sedimentary Petrology*, **53**, 521–532.

975 **Bourillot, R., Vennin, E., Dupraz, C., Pace, A., Foubert, A., Rouchy, J.-M., Patrier, P.,**  
976 **Blanc, P., Bernard, D., Lesseur, J. and Visscher, P.T.** (2020) The Record of  
977 Environmental and Microbial Signatures in Ancient Microbialites: The Terminal Carbonate  
978 Complex from the Neogene Basins of Southeastern Spain. *Minerals*, **10**, 276.  
979 DOI.org/10.3390/min10030276

980 **Bowerbank, J.S.** (1862) On the Anatomy and Physiology of the Spongiadae. Part III. On the  
981 Generic Characters, the Specific Characters, and on the Method of Examination.  
982 *Philosophical Transactions of the Royal Society of London*, **152**, 1087-1135.

983 **Brachert, T.C., Dullo, W.C. and Stoffers, P.** (1987) Diagenesis of siliceous sponge  
984 limestones from the Pleistocene of the Tyrrhenian sea (Mediterranean sea). *Facies*, **17**,  
985 41–49.

986 **Brayard, A., Vennin, E., Olivier, N., Bylund, K.G., Jenks, J., Stephen, D.A., Bucher, H.,**  
987 **Hofmann, R., Goudemand, N. and Escarguel, G.** (2011) Transient metazoan reefs in the  
988 aftermath of the end-Permian mass extinction. *Nature Geoscience*, **4**, 693–697.

989 **Bromley R.G. and Schönberg C.H.** (2008) Borings, bodies and ghosts: spicules of the  
990 endolithic sponge *Aka akis* sp. nov. within the boring *Entobia cretacea*, Cretaceous,

- 991 England. In: *Current Developments in Bioerosion* (eds Wisshak M., Tapanila L.), Erlangen  
992 Earth Conference Series. Springer, Berlin, Heidelberg. [https://doi.org/10.1007/978-3-540-](https://doi.org/10.1007/978-3-540-77598-0_12)  
993 [77598-0\\_12](https://doi.org/10.1007/978-3-540-77598-0_12).
- 994 **Butterfield, N. J. and Nicholas, C. J.** (1996) Burgess Shale-type preservation of both non-  
995 mineralizing and 'shelly' Cambrian organisms from the Mackenzie Mountains,  
996 northwestern Canada. *Journal of Paleontology*, **70**, 893-899.  
997 DOI:10.1017/s0022336000038579.
- 998 **Cloud, P.** (1973) Pseudofossils: a plea for caution. *Geology*, **1**, 123-127.
- 999 **Conway Morris, S. and Whittington, H.B.**, 1985, Fossils of the Burgess Shale. *Geological*  
1000 *Survey of Canada, Miscellaneous Reports*, **43**, 1-31.
- 1001 **Debrenne, F.** (1999) The past of sponges, sponges of the past. *Memoirs of the Queensland*  
1002 *Museum*, **44**, 9-21.
- 1003 **Debrenne, F., Gandin, A., and Rowland, S.M.** (1989) Lower Cambrian bioconstructions in  
1004 Northwestern Mexico (Sonora). Depositional setting, paleoecology and systematics of  
1005 Archaeocyaths, *Geobios*, **22**, 137-195.
- 1006 **de Voogd, N.J., Alvarez, B., Boury-Esnault, N., Carballo, J.L., Cárdenas, P., Díaz, M.-C.,**  
1007 **Dohrmann, M., Downey, R., Hajdu, E., Hooper, J.N.A., Kelly, M., Klautau, M.,**  
1008 **Manconi, R., Morrow, C.C., Pisera, A.B., Ríos, P., Rützler, K., Schönberg, C., Vacelet,**  
1009 **J. and van Soest, R.W.M.** (2022). World Porifera Database:  
1010 <https://www.marinespecies.org/>.
- 1011 **Dickson J.A.D.** (1978) Neomorphism and recrystallization. In: *Encyclopedia of Sediments*  
1012 *and Sedimentary Rocks* (Eds G.V. Middleton, M. J. Church, M. Coniglio, L.A. Hardie, F.J.  
1013 Longstaffe). Encyclopedia of Earth Sciences Series. Springer, Dordrecht.  
1014 DOI.org/10.1007/978-1-4020-3609-5\_143 (2003 edition).
- 1015 **Ehrlich, H., Rigby, J. K., Botting, J. P., Tsurkan, M. V., Werner, C., Schwille, P., Petrasek,**  
1016 **Z., Pisera, A., Simon, P., Sivkov, V. N., Vyalikh, D. V., Molodtsov, S. L., Kurek, D.,**  
1017 **Kammer, M., Hunoldt, S., Born, R., Stawski, D., Steinhof, A., Bazhenov, V. V., and**  
1018 **Geisler, T.** (2013) Discovery of 505-million-year old chitin in the basal demosponge  
1019 *Vauxia gracilentia*. *Scientific Reports*, **3**, 3497; DOI: 10.1038/srep03497.
- 1020 **Ehrlich, H.** (2019) Marine Biological Materials of Invertebrate Origin. Springer. 329pp.
- 1021 **Ellison, A. M., Farnsworth, E. J. and Twilley, R. R.** (1996) Facultative mutualism between  
1022 red mangroves and root-fouling sponges in Belizean mangal. *Ecology*, **77**, 2431-2444.
- 1023 **Erpenbeck, D., Sutcliffe, P., Cook, S., Dietzel, A., Maldonado, M., van Soest, R.W.M.,**  
1024 **Hooper, J.N.A. and Wörheide, G.** (2012) Horny sponges and their affairs: on the  
1025 phylogenetic relationships of keratose sponges. *Molecular Phylogenetics and Evolution*,  
1026 **63**, 809-816.
- 1027 **Exposito, J.-Y., Le Guellec, D., Lu, Q. and Garrone, R.** (1991) Short chain collagens in  
1028 sponges are encoded by a family of closely related genes. *The Journal of Biological*  
1029 *Chemistry*, **266**, 21923-21928.
- 1030 **Ezaki, Y., Liu, J., Nagano, T. and Adachi, N.** (2008) Geobiological aspects of the earliest  
1031 Triassic microbialites along the southern periphery of the tropical Yangtze Platform:  
1032 initiation and cessation of a microbial regime. *Palaios*, **23**, 356-369.
- 1033 **Fan, W., Zhao, Y., Chen, A., You X. and Cong, P.** (2021) New vauxiid sponges from the  
1034 Chengjiang Biota and their evolutionary significance. *Journal of the Geological Society*,  
1035 **178**, jgs2020-162.
- 1036 **Flügel, E.** (2004) *Microfacies in Carbonate Rocks; analysis, interpretation and application*.  
1037 Springer, Berlin, Heidelberg, New York. 976 pp.
- 1038 **Flügel, E. and Munnecke, A.** (2010) Microfacies of carbonate rocks: analysis, interpretation  
1039 and application. Springer, Heidelberg, New York.
- 1040 **Foster, W. J., Heindel, K., Richoz, S., Gliwa, J., Lehrmann, D. J., Baud, A., Kolar-**  
1041 **Jurkovsek, T., Aljinovic, D., Jurgovsek, B., Korn, D., Martindale, R.C. and Peckmann,**



- 042 **J.** (2019) Suppressed competitive exclusion enabled the proliferation of Permian/Triassic  
043 boundary microbialites. *Depositional Record*, **2020**, 62–74. DOI: 10.1002/dep2.97.
- 044 **Friesenbichler, E., Richoz, S., Baud, A., Krystyn, L., Sahakyan, L., Vardanyan, S.,**  
045 **Peckmann, J., Reitner, J. and Heindel, K.** (2018) Sponge-microbial buildups from the  
046 lowermost Triassic Chanakhchi section in southern Armenia: microfacies and stable  
047 carbon isotopes. *Palaeogeography Palaeoclimatology Palaeoecology*, **490**, 653–672.
- 048 **Fritz, G.K.** (1958) Schwammstotzen, Tuberolithe und Schuttbreccien im Weißen Jura der  
049 Schwäbischen Alb. *Arbeiten aus dem Geologisch–Palaontologischen Institut der*  
050 *Technischen Hochschule, Stuttgart, Neue Folge*, **13**, 1–119.
- 051 **Froget, C.** (1976) Observations sur l'altération de la silice et des silicates au cours de la  
052 lithification carbonatée (Région Siculo-Tunisienne). *Géologie Méditerranéenne*, **3**, 219–  
053 225.
- 054 **Gazave, E., Lapébie, P., Ereskovsky, A., Vacelet, J., Renard, E., Cardenas, P. and**  
055 **Borchiellini, C.** (2012) No longer Demospongiae: Homoscleromorph formal nomination as  
056 a fourth class of porifera. *Hydrobiologia*, **687**, 3 - 10.
- 057 **Gischler, E., Fuchs, A., Bach, W. and Reitner, J.** (2021) Massive cryptic microbe-sponge  
058 deposits in a Devonian fore-reef slope (Elbingerode Reef Complex, Harz Mts., Germany).  
059 *PalZ*, DOI.org/10.1007/s12542-021-00581-8.
- 060 **Göthel, H.** (1992) Guide de la faune sous-marine: La Méditerranée. Invertébrés marins et  
061 poissons. Eygen Ulmer GmbH & Co. 318 pp.
- 062 **Gray, J.E.** (1867) Notes on the Arrangement of Sponges, with the Descriptions of some New  
063 Genera. *Proceedings of the Zoological Society of London*. **2**, 492-558, pls XXVII-XXVIII.
- 064 **Grotzinger, J. and Rothman, D.** (1996) An abiotic model for stromatolite morphogenesis.  
065 *Nature* **383**, 423–425.
- 066 **Gupta N.S. and Briggs D.E.G.** (2011) Taphonomy of Animal Organic Skeletons Through  
067 Time. In: Taphonomy. Aims & Scope (Eds P.A. Allison, D.J. Bottjer) Topics in Geobiology  
068 Book Series, vol 32. Springer, Dordrecht.
- 069 **Gutzmer, J., Schaefer, M. O. and Beukes, N. J.** (2002) Red bed-hosted oncolitic  
070 manganese ore of the Paleoproterozoic Soutpansberg Group, Bronkhorstfontein, *South*  
071 *Africa. Economic Geology*, **97**, 1151-1166.
- 072 **Gürich, G.** (1906) Les spongiostromides du Viséen de la Province de Namur. *Memoirs of the*  
073 *Royal Belgian Museum of Natural Sciences*, **3**, 1–55.
- 074 **Heindel, K., Foster, W. J., Richoz, S., Birgel, V. J., Roden, D., Baud, A., Brandner, R.,**  
075 **Krystyn, L., Mohtat, T., Kosun, E., Twitchett, R., Reitner, J. and Peckmann, J.** (2018)  
076 The formation of microbial-metazoan bioherms and biostromes following the latest Permian  
077 mass extinction. *Gondwana Research*, **61**, 187–202.
- 078 **Hofmann, H.J.** (1972) Precambrian remains in Canada: fossils, dubiofossils, and  
079 pseudofossils. *International Geological Congress, 24th Session, Montreal, Proceedings of*  
080 *Section 1*, p. 20-30.
- 081 **Jenner, R.A. and Littlewood, D.T.J.** (2008) Problematica old and new. *Philosophical*  
082 *Transactions of the Royal Society, London, B, Biological Sciences*, **363**, 1503–1512.
- 083 **Kamenskaya, O.E., Gooday, A.J., Tendal, O.S. and Melnik, V.F.** (2015) Xenophyophores  
084 (Protista, Foraminifera) from the Clarion-Clipperton Fracture Zone with description of three  
085 new species. *Marine Biodiversity* **45**, 581–593.
- 086 **Kenny, N.J., Francis, W.R., Rivera-Vicéns, R.E., Juravel, K., de Mendoza, A., Díez-Vives,**  
087 **C., Lister, R., Bezares-Calderón, L. A., Grombacher, L., Roller, M., Barlow, L., Camilli,**  
088 **S., Ryan, J., Wörheide, G., Hill, A., Riesgo, A. and Leys, S.** (2020) Tracing animal  
089 genomic evolution with the chromosomal-level assembly of the freshwater sponge  
090 *Ephydatia muelleri*. *Nature Communications* **11**, 3676.
- 091 **Kershaw, S.** (2000) Quaternary reefs of northeastern Sicily: structure and growth controls in  
092 an unstable tectonic setting. *Journal of Coastal Research*, **16**, 1037-1062.

- 109 **Kershaw, S., Guo, L. and Braga, J-C.** (2005) A Holocene coral-algal reef at Mavra Litharia,  
1094 Gulf of Corinth, Greece: structure, history and applications in relative sea-level change.  
1095 *Marine Geology*, **215**, 171-192.
- 1096 **Kershaw, S., Li, Q., and Li, Y.** (2021a) Addressing a Phanerozoic carbonate facies  
1097 conundrum—sponges or clotted micrite? Evidence from Early Silurian reefs, South China  
1098 Block. *The Sedimentary Record*, **19**, 3-10.
- 1099 **Kershaw, S., Zhang, T. and Li, Y.** (2021b) *Calcilobes wangshenghaii* n. gen., n. sp.,  
1100 microbial constructor of Permian-Triassic boundary microbialites of South China, and its  
1101 place in microbialite classification. *Facies*, **67**:28.
- 1102 **Knaust, D.** (2007) Invertebrate trace fossils and ichnodiversity in shallow-marine carbonates  
1103 of the German Middle Triassic (Muschelkalk). In: *Sediment-Organism Interactions: A*  
1104 *Multifaceted Ichnology* (Ed. R. G. Bromley) *SEPM Special Publication*, **88**, 223-240.
- 1105 **Knaust, D.** (2010) Meiobenthic trace fossils comprising a miniature ichnofabric from Late  
1106 Permian carbonates of the Oman Mountains. *Palaeogeography, Palaeoclimatology,*  
1107 *Palaeoecology*, **286**, 81-87.
- 1108 **Knoll, A.H.** (2003) Biomineralization and Evolutionary History. *Reviews in Mineralogy and*  
1109 *Geochemistry*, **54**, 329–356. DOI.org/10.2113/0540329
- 1110 **Kris, A. and McMenamin, M.A.S.** (2021) Putative Proterozoic sponge spicules reinterpreted  
1111 as microburrows. *Academia Letters*, Article 3800. <https://doi.org/10.20935/AL3800>.
- 1112 **Kuang, H-W.** (2014) Review of molar tooth structure research. *Journal of Palaeogeography*, **3**,  
1113 359-383.
- 1114 **Lakshatanov, L.Z. and Stipp, S.L.S.** (2010) Interaction between dissolved silica and calcium  
1115 carbonate: 1. Spontaneous precipitation of calcium carbonate in the presence of dissolved  
1116 silica, *Geochimica et Cosmochimica Acta*, **74**, 2655-2664.
- 1117 **Lee, J.-H. and Hong, J.** (2019) Sedimentologic and paleoecologic implications for keratose-  
1118 like sponges in geologic records. *Journal of the Geological Society of Korea*. **55**, 735-748.
- 1119 **Lee, J.-H. and Riding, R.** (2020) The ‘classic stromatolite’ *Cryptozoön* is a keratose sponge-  
1120 microbial consortium. *Geobiology*, **19**, 189-198. DOI: 10.1111/gbi.12422.
- 1121 **Lee, J.-H. and Riding, R.** (2021a) Keratolite–stromatolite consortia mimic domical and  
1122 branched columnar stromatolites, *Palaeogeography, Palaeoclimatology, Palaeoecology*,  
1123 **571**, 10288.
- 1124 **Lee, J.-H. and Riding, R.** (2021b) The ‘classic stromatolite’ *Cryptozoön* is a keratose sponge-  
1125 microbial consortium. *Geobiology*, **19**, 189–198.
- 1126 **Lee, J.-H., Chen, J., Choh, S-J., Lee, D-J., Han, Z. and Chough, S.K.** (2014) Furongian (late  
1127 Cambrian) sponge-microbial maze-like reefs in the North China Platform. *Palaios*, **29**, 27-  
1128 37.
- 1129 **Lees, A. and Miller, J.** (1995) Waulsortian banks. In: *Carbonate Mud-Mounds, Their Origin*  
1130 *and Evolution* (Ed. C.L.V. Monty, D.W.J. Bosence, P.H. Bridges and B.R. Pratt), Special  
1131 Publications of the International Association of Sedimentologists, **23**, 191-271.
- 1132 **Löhr S. C. and Kennedy M. J.** (2015) Micro-trace fossils reveal pervasive reworking of  
1133 Pliocene sapropels by low-oxygen-adapted benthic meiofauna. *Nature Communications*,  
1134 **6**, 1–8.
- 1135 **Lokier, S.W. and Al Junaibi, M.** (2016) The petrographic description of carbonate facies: are  
1136 we all speaking the same language? *Sedimentology*, **63**, 1843–1885.
- 1137 **Love, G.D., Grosjean, E., Stalvies, C., Fike, D. A., Grotzinger, J. P., Bradley, A. S.,**  
1138 **Kelly, A. E., Bhatia, M., Meredith, W., Snape, C. E., Bowring, S. A., Condon, D.**  
1139 **J. and Summons, R. E.** (2009) Fossil steroids record the appearance  
1140 of Demospongiae during the Cryogenian period. *Nature* **457**, 718–721.
- 1141 **Luo, C. and Reitner, J.** (2014) First report of fossil “keratose” demosponges in Phanerozoic  
1142 carbonates: Preservation and 3-D reconstruction. *Naturwissenschaften*, **101**, 467–477.

- 143 **Luo, C. and Reitner, J.** (2016) 'Stromatolites' built by sponges and microbes—a new type of  
144 Phanerozoic bioconstruction. *Lethaia*, **49**, 555–570.
- 145 **Mcllroy, D.** (2022) Were the first trace fossils really burrows or could they have been made by  
146 sediment-displacive chemosymbiotic fossils? *Life*, **12**, 136. <https://doi.org/10.3390/life12020136>.
- 148 **McMahon, S., Hood, A. and Mcllroy, D.** (2017) Origin and occurrence of subaqueous  
149 sedimentary cracks. In: *Earth System Evolution and Early Life: A Celebration of the Work*  
150 *of Martin Brasier*. Brasier, A. T., Mcllroy, D. & McLoughlin, N. (eds). Geological Society,  
151 London, Special Publications, **448**, 285-309.
- 152 **McMahon, S. and Cosmidis, J.** (2021) False biosignatures on Mars: anticipating ambiguity.  
153 *Journal of the Geological Society* 2021; DOI.org/10.1144/jgs2021-050
- 154 **McMahon, S., Ivarsson, M., Wacey, D., Saunders, M., Belivanova, V., Muirhead, D., Knoll,  
155 P., Steinbock, O. and Frost, D.A.** (2021) Dubiofossils from a Mars-analogue subsurface  
156 palaeoenvironment: the limits of biogenicity criteria. *Geobiology*, DOI: 10.1111.gbi.12445.
- 157 **McMenamin, M.A.S.** (2016) Parenting skills. In McMenamin, M.A.S. *Dynamic Paleontology:  
158 Using Quantification and Other Tools to Decipher the History of Life*. Springer, Cham,  
159 Switzerland, pp 191-205.
- 160 **Macintyre, I.G.** (1985) Submarine cements—the peloidal question. *SEPM Special Publication*  
161 **36**, 109–116.
- 162 **Manconi, R., Cadeddu, B., Ledda, F. and Pronzato, R.** (2013) An overview of the  
163 Mediterranean cave-dwelling horny sponges (Porifera, Demospongiae).- *ZooKeys*, **281**, 1-  
164 68.
- 165 **Matysik, M.** (2016) Facies types and depositional environments of a morphologically diverse  
166 carbonate platform: a case study from the Muschelkalk (Middle Triassic) of Upper Silesia,  
167 southern Poland. *Annales Societatis Geologorum Poloniae*, **86**, 119-164.
- 168 **Monty, C.** (1981) Phanerozoic Stromatolites: case histories. Springer-Verlag, Berlin,  
169 Heidelberg, New York, 249pp.
- 170 **Morrow, C. and Cárdenas, P.** (2015) Proposal for a revised classification of the  
171 Demospongiae (Porifera). *Frontiers in Zoology*, **12**:7. 27 pages. DOI 10.1186/s12983-015-  
172 0099-8.
- 173 **Neuweiler, F., Gautret, P., Thiel, V., Lange, R., Michaelis, W. and Reitner, J.** (1999)  
174 Petrology of Lower Cretaceous carbonate mud mounds (Albian, N. Spain): insights into  
175 organomineralic deposits of the geological record: *Sedimentology*, **46**, 837–859.
- 176 **Neuweiler, F., Daoust, I., Bourque, P.-A. and Burdige, J.B.** (2007) Degradative calcification  
177 of a modern siliceous sponge from the Great Bahama Bank, the Bahamas: A guide for  
178 interpretation of ancient sponge-bearing limestones: *Journal of Sedimentary Research*, **77**,  
179 552–563.
- 180 **Neuweiler, F., Turner, E.C. and Burdige, D.J.** (2009) Early Neoproterozoic origin of the  
181 metazoan clade recorded in carbonate rock texture. *Geology*, **37**, 475–478.
- 182 **Park, J., Lee, J.-H., Hong, J., Choh, D.-C. and Lee, D.-J.** (2015) An Upper Ordovician sponge-  
183 bearing micritic limestone and implication for early Palaeozoic carbonate successions.  
184 *Sedimentary Geology*, **319**, 124-133.
- 185 **Park, J., Lee, J.-H., Hong, J., Choh, S.-J., Lee, D.-C. and Lee, D.-J.** (2017) Crouching  
186 shells, hidden sponges: Unusual Late Ordovician cavities containing sponges.  
187 *Sedimentary Geology*, **347**, 1–9.
- 188 **Pei, Y., Duda, J.-P., Schönig, J., Luo, C. and Reitner, J.** (2021a) Late Anisian microbe-  
189 metazoan build-ups in the Germanic Basin: aftermath of the Permian-Triassic crisis.  
190 *Lethaia*, 10.1111/let.12442.
- 191 **Pei, Y., Hagdorn, H., Voigt, T., Duda, J.-P. and Reitner, J.** (2021b) Palaeoecological  
192 implications of Lower-Middle Triassic stromatolites and microbe-metazoan build-ups in the

- 193 Germanic Basin: insights into the aftermath of the Permian-Triassic crisis. *Geosciences*,  
194 **12**, 133. <https://doi.org/10.3390/geosciences12030133>.
- 195 **Pemberton, S.G. and Gingras, M.K.** (2005) Classification and characterizations of  
196 biogenically enhanced permeability. *American Association of Petroleum Geologists*  
197 *Bulletin*, **89**,1495-1517.
- 198 **Pham, D., Hong, J. and Lee, J.H.** (2021) Keratose sponge–microbial consortia in  
199 stromatolite-like columns and thrombolite-like mounds of the Lower Ordovician  
200 (Tremadocian) Mungok Formation, Yeongwol, Korea.- *Palaeogeography,*  
201 *Palaeoclimatology, Palaeoecology*, **572**, 110409.
- 202 **Pisera, A.** (1997) Upper Jurassic Siliceous Sponges from the Swabian Alb: Taxonomy and  
203 Paleocology. *Palaeontologia Polonica*, **57**, 3-216.
- 204 **Reitner, J.** (1993) Modern cryptic microbialite/metazoan facies from Lizard Island (Great  
205 Barrier Reef, Australia) formation and concepts. *Facies*, **29**, 3–39.
- 206 **Reitner, J. and Keupp, H.** (1991) The fossil record of the Haplosclerid excavating sponge  
207 *Aka de Laubenfels*. In: *Fossil and Recent Sponges*. (Eds J. Reitner and H. Keupp, H.)  
208 Springer-Verlag, Berlin, Heidelberg, 102-120.
- 209 **Reitner, J. and Wörheide, G.** (2002). Non-lithistid fossil Demospongiae: origins of their  
210 palaeobiodiversity and highlights in history of preservation, In: *Systema Porifera: a guide*  
211 *to the classification of Sponges* (Eds J.N.A. Hooper and R.W.M. van Soest) Kluwer  
212 Academic/Plenum Publishers, New York, 52-68.
- 213 **Reitner, J., Hühne, C. and Thiel, V.** (2001) Porifera-rich mud mounds and microbialites as  
214 indicators of environmental changes within the Devonian/Lower Carboniferous critical  
215 interval. *Terra Nostra*, **4**, 60-65.
- 216 **Retallack, G.J.** (2015) Reassessment of the Silurian problematicum *Rutgersella* as another  
217 post-Ediacaran vendobiont, *Alcheringa*, **39**, 573-588. DOI:  
218 10.1080/03115518.2015.1069483.
- 219 **Rigby, J.K., Rohr, D.M., Blodgett, R.B. and Britt, B.B.** (2008) Silurian sponges and some  
220 associated fossils from the Heceta Limestone, Prince of Wales Island, southeastern  
221 Alaska. *Journal of Paleontology*, **82**, 91-101.
- 222 **Ruetzler, K. and Richardson, S.** (1996) The Caribbean spicule tree: a sponge-imitating  
223 foraminifer (Astrorhizidae). *Bulletin de l'Institut Royal des Sciences Naturelles de Belgique,*  
224 *Biologie supplement*, **66**,143–151.
- 225 **Semprucci, F. and Sandulli, R.** (eds) (2020) *Meiofauna Biodiversity and Ecology*. MDPI,  
226 Basel. 241 pp.
- 227 **Schaefer, M.O., Gutzmer, J. and Beukes, N.J.** (2001) Late Paleoproterozoic Mn-rich  
228 oncoids: Earliest evidence for microbially mediated Mn precipitation. *Geology*, **29**, 835–  
229 838.
- 230 **Schieber, J., Southard, J.B., Kissling, P., Rossman, B. and Ginsburg, R.** (2013)  
231 Experimental Deposition of Carbonate Mud From Moving Suspensions: Importance of  
232 Flocculation and Implications For Modern and Ancient Carbonate Mud Deposition. *Journal*  
233 *of Sedimentary Research*, **83**, 1026–1032.
- 234 **Schuster, A., Vargas, S., Knapp, I.S., Pomponi, S. A, Toonen, R. J., Erpenbeck, D. and**  
235 **Wörheide, G.** (2018) Divergence times in demosponges (Porifera): first insights from new  
236 mitogenomes and the inclusion of fossils in a birth-death clock model. *BMC Evol Biol* **18**,  
237 114. <https://doi.org/10.1186/s12862-018-1230-1>.
- 238 **Scoffin, T.P.** (1987) *An Introduction to Carbonate Sediments and Rocks*. Blackie, Glasgow  
239 and London, 274pp.
- 240 **Servais, T., Cascales-Minana, B. and Harper, D.A.T.** (2021) The Great Ordovician  
241 Biodiversification Event (GOBE) is not a single event. *Paleontological Research*, **25**, 315-  
242 328.

- 243 **Shen, Y. and Neuweiler, F.** (2018) Questioning the microbial origin of automicrite in  
244 Ordovician calathid–demosponge carbonate mounds. *Sedimentology*, **65**, 303–333
- 245 **Shinn, E.A.** (1968) Practical significance of birdseye structures in carbonate rocks. *Journal of*  
246 *Sedimentary Petrology*, **38**, 215–223.
- 247 **Stocchino, G.A., Cubeddu, T., Pronzato, R., Sanna, M.A. and Manconi, R.** (2021) Sponges  
248 architecture by colour: new insights into the fibres morphogenesis, skeletal spatial layout  
249 and morpho-anatomical traits of a marine horny sponge species (Porifera), *The European*  
250 *Zoological Journal*, **88**, 237–253.
- 251 **Stock, C. W. and Sandberg, C.A.** (2019) Latest Devonian (Famennian, *expansa* Zone)  
252 conodonts and sponge-microbe symbionts in Pinyon Peak Limestone, Star Range,  
253 southwestern Utah, lead to reevaluation of the global Dasberg Event. *Palaeogeography,*  
254 *Palaeoclimatology, Palaeoecology*, **534**, 109271.
- 255 **Szulc, J.** (1997) Middle Triassic (Muschelkalk) sponge-microbial stromatolites, diplopores and  
256 Girvanella-encrustations from the Silesian Cracow Upland. In: 3rd IFAA Regional Symposium  
257 and IGCP 380 International Meeting, Guidebook. Cracow, pp 10–15.
- 258 **Tucker, M.E. and Wright, V.P.** (1990) *Carbonate Sedimentology*. Blackwell Scientific  
259 Publications, Oxford, London.
- 260 **Turner, E.C.** (2021) Possible poriferan body fossils in early Neoproterozoic microbial reefs.  
261 *Nature*, **596**, 87–91.
- 262 **Turner, E.C., James, N.P. and Narbonne, G.M.** (2000) Taphonomic control on microstructure  
263 in early Neoproterozoic reefal stromatolites and thrombolites: *Palaios*, **15**, 87–111.
- 264 **Walcott, C. D.** (1917) Middle Cambrian Spongiae. *Smithsonian Miscellaneous Collections*, **67**  
265 (6), 261–364.
- 266 **Wallace, M.W., Hood, A.V.S., Woon, E.M.S., Hoffmann, K.-H. and Reed, C.P.** (2014)  
267 Enigmatic chambered structures in Cryogenian reefs: the oldest sponge-grade organisms?  
268 *Precambrian Research*, **255**, 109–123.
- 269 **Wiedenmayer, F.** (1978) Modern sponge bioherms of the Great Bahama Bank: *Eclogae*  
270 *Geologicae Helveticae*, **71**, 699–744.
- 271 **Wood, R.** (2016) Palaeoecology of Ediacaran metazoan reefs. In: *Earth System Evolution and*  
272 *Early Life: a celebration of the Work of Martin Brasier* (Eds A.T. Brasier, D. McIlroy and N.  
273 McLoughlin) Geological Society, London, Special Publications, 448,  
274 <http://doi.org/10.1144/SP448.1>, 195–210.
- 275 **Wood, R., Zhuravlev, A.Y. and Anaaz, C.T.** (1993) The ecology of Lower Cambrian buildups  
276 from Zuune Arts, Mongolia: implications for early metazoan reef evolution. *Sedimentology*,  
277 **40**, 829–858. <https://doi.org/10.1111/j.1365-3091.1993.tb01364.x>
- 278 **Wörheide G.** (2008) A hypercalcified sponge with soft relatives: *Vaceletia* is a keratose  
279 demosponge. *Molecular and Phylogenetic Evolution*, **47**, 433–438.
- 280 **Wright, V.P. and Barnett, A.J.** (2020) The textural evolution and ghost matrices of the  
281 Cretaceous Barra Velha Formation carbonates from the Santos Basin, offshore Brazil.  
282 *Facies*, **66**, 7. <https://doi.org/10.1007/s10347-019-0591-2>.
- 283 **Wu, S., Chen, Z.-Q., Su, C., Fang, Y. and Yang, H.** (2021) Keratose sponge fabrics from the  
284 lowermost Triassic microbialites in South China: geobiologic features and Phanerozoic  
285 evolution. *Global and Planetary Change*, <https://doi.org/10.1016/j.gloplacha.2022.103787>.
- 286 **Wulff, J.** (2016) Sponge contributions to the geology and biology of reefs: past, present and  
287 future. In: *Coral reefs at the Crossroads* (Eds D.K. Hubbard et al.). Coral reefs of the World  
288 6. Springer Science + Business Media Dordrecht, 103–126. DOI 10.1007/978-94-017-7567-  
289 0\_5.
- 290 **Zheng, L.J., Jiang, H.X., Wu, Y.S., H-P., Zhang, Y.-Y., Ren, J.-F. and Huang, Z.-L.** (2020)  
291 *Halysia* Høeg, 1932 — an ancestral tabulate coral from the Ordos Basin, North China.  
292 *Journal of Palaeogeography*, **9**, 26. [doi.org/10.1186/s42501-020-00073-x](https://doi.org/10.1186/s42501-020-00073-x)  
293

294

295

296

297 **Table S1** – Compilation of publications describing possible keratose sponges, presented  
 298 in stratigraphic order (oldest at bottom), together with key points and interpretive  
 299 comments by the authors of this study; the list of references in the table is provided below  
 300 the table.>>>

Reference	Age and Context	Fabric element; Discussion	Conclusion	Comments
Luo, 2015	PhD thesis	Source document for Luo & Reitner 2014, 2016, and also includes a chapter on keratosa through geological time		Chapters give source figures for those two papers, and the keratosa-through-time section shows vermiform fabrics with no verification of sponges.
Monty, 1981	Review; revision of terminology (Pia, 1927)	Spongiostromate microstructure to result from the individualization of micritic, spongioid, fenestral, sparitic, pelloidal, detrital, etc. laminae or films, variously grouped and organized.	Bacterial in origin. Variation in function of the environment and taphonomy	Replaces “cryptalgal”; spongiostromate microstructure is common in Precambrian stromatolites and oncolites
Wolf, 1965b	Review; revision of terminology	Fecal vs. algal pellets; orthomicrite vs pseudomicrite allomicrite vs automicrite orthosparite vs pseudosparite	In-situ growth vs. accumulation of algal degradation products	Porostromata vs. Pseudostromata (Table-II). Allomicrite and automicrite
Pratt, 1982	Phanerozoic mud-mounds	Fig. 13-15: Distinction between vermiform and spongiform microstructures	Cryptalgal; microbial; molds of filaments; burrowing	Vermiform in ref. to Ross et al.,(1975) and Kapp (1975, Fig 3). Spongiform= spongiostromata + burrows
Luo and Reitner, 2014	Triassic microbialite	Fig, 3: Laminated birdseye limestone, some fenestrae	Putative keratose sponge	No verification of a keratose origin
Brayard et al., 2011; but see also Brayard et al., 2017.	L. Triassic bioaccumulations and reefs	Fig.3; Supp. Fig.2: Spheroid, encrusting sponges, no specific wall structure. Very thin spicules (non-fused).	lyssacine hexactinellids, Calcareae?	Considered keratose sponges by Lee & Riding (2021). Similar to vermiform, spongiform, vuggy and fenestral microstructures
Adachi et al., 2017	L. Triassic stromatolites	Displays clotted structures. The word “spongy” appears once, but no link to sponges; neither “sponge”	Erroneously included in Lee & Riding 2021, table 1; Adachi et al have not	

		nor “keratose” nor “spicule” appear in this paper	indicated a sponge content in their study.	
Baud et al., 2021	L. Triassic buildups after mass extinction.	Network structures between digitate stromatolites and sea-floor sparite masses. No good detailed pictures	No justification for conclusion of a “sponge takeover” after end-Permian mass extinction	Cannot be assessed because quality of images too poor
Friesenbichler et al., 2018	Basal Triassic, Armenia	“Basal Triassic Sponge-Microbial Buildups.”. Network structures between digitate stromatolites Fig. 10B: network elements at margin of network lie parallel to margins, might be expected in a sponge. Structures in Fig. 10 do look like they could be sponges, but the problem is verification.	Sponge stated as being “interpreted” but overall message is sponges are really present, thus self-contradiction.	P654, LH, para 1, lines 5-10: 1 <sup>st</sup> sentence says “interpreted as sponges”; 2 <sup>nd</sup> sentence drops the “interpreted” giving impression they are definite sponges. The whole paper does not provide verification of sponges, so these basal Triassic microbialite buildups don’t have confirmed sponges. Also inaccurate literature citation supporting interpretation of sponges (See separate file called: “FriesenbichlerEtAl2018 -SpongeNotes-SK”)
Heindel et al., 2018	Permian-Triassic boundary, Iran & Turkey	Sponge-microbial constructions. “Possible keratose sponges”	Despite calling them “possible keratose sponges”, authors really want these to be sponges	ALL the photos of claimed “possible keratose sponges” are insufficient quality to allow any judgement about whether or not they are sponges
Luo and Reitner, 2016	Carboniferous & Triassic stromatolites	Reinterpreted as sponge-microbial buildups . . “previously reported fossils of keratose sponges”. Compares with modern keratose sponges from Lizard Island that have excurrent canals; similar spaces seen in fossil examples but their origin is equivocal, cos occupied by shelly fossils and thus may be borings.	Keratose sponges combined with microbial micrite as buildups.	P1 RH, bottom of page, to p2, LH, top of page: Assumes keratose origin to have been proven, but does not demonstrate verification of keratose sponges.

Gürich, 1906	Carboniferous (Viséan)	*Establishes the term “ <i>spongiostromides</i> ” (spongiostromata). Five categories and fourteen specific microfabrics (genus and species level)	Product of excretion by rhizopods (Xenophyophores)	Spongiostromata with 14 morphospecies (crusts and oncoids)
Kaisin, 1922	Carboniferous (Viséan)	“Structure grumeleuse”	Flocculation of sapropelic sediments	These clots may be the center of oolites or pisolites
Kaisin, 1925	Carboniferous (Viséan)	“Structure grumeleuse”	Bacterial origin	
Cayeux, 1935	Carboniferous (Viséan, Coal measures)	“Structure grumeleuse” (Pl XVIII) “Structure vermiculée”, “structure spongieuse”	Aggrading neomorphism Decay of plant debris	Grumous texture, radial recrystallisation
Rodríguez-Martínez et al., 2012	Carboniferous microbial mud mound derived boulders	No detailed or systematic mentioning of carbonate microstructures	No conclusions about carbonate microstructures	Referenced in Lee & Riding (2021) as a Cretaceous (Turonian) “keratose sponge”.
Schwarzacher, 1961	L. Carboniferous knoll-reefs	Pelleted, clotted, flocculent textures (incl. <i>Spongiostroma</i> )	Unresolved (detrital, fecal, algal)	Refers to Hadding (1959)
Lees, 1964	L. Carboniferous (Waulsortian)	Multicomponent mudstone. Patches of flocculent, pelleted or clotted material	Algae, sponges; disintegration, baffling	M1, (M2); syndepositional lithification and collapse
Tsien, 1985	U. Devonian mud-mounds	Different types of micrite in mud-mounds: “spongy structure” and “peloidal structure” (Figs 2 & 3)	Unresolved	In-situ microbial production of micrite in mud-mounds
Zhou and Pratt, 2019	U. Devonian	Copious illustration of clotted fabrics and peloids described as sponge networks; includes cavities in clotted micrite masses, cavities are geopetal with peloids and clotted micrites in the cavities, but these are described as sponges	Sponges are a key component of these sediments	Authors seem convinced of a prominent sponge component, but there is no description of criteria for sponges; all the illustrated examples may be simply clotted micrites and peloids.
Stock and Sandberg, 2019	Famennian, SW Utah	1m-thick sponge-microbe bed, part of Dasberg Event, and considered related to extinction. Interlayered stromatolite and clotted fabric attributed to sponges. Details in Figs 6&7	Claim of canals in the sponges (Fig. 6) but not clear on photo.	Cites Luo & Reitner (2014, 2016) as basis for interpretation. Described structures resemble keratolite fabrics, but there is no verification of sponges here.
Luo and Reitner, 2014	Devonian reef mound	Fig. 2a, f: Microproblematicum with translucent sclerites.	Putative keratose sponge	No verification a keratose origin



Luo and Reitner, 2014	Devonian reef mound	Fig. 2e, g: Geopetal fill; compaction of peloids,.	Putative keratose sponge	No verification a keratose origin
Wolf, 1965a	L. Devonian algal-reef complex	Calcilutites of dense, grumous, cellular, tubular, “pelletoid” and “granuloid” textures; algal crusts (poro- vs pseudo- or spongiostromata); stromatolites, birdseyes.	Algal reefs, algae and their byproducts	Pseudostromata (=spongiostromata), Porostromata = filaments, tubes, cells (Pia, 1927)
Clough and Blodgett, 1989	Silurian/Devonian algal reef complex	Fig. 3: Vermiform microstructure in thrombolite mud mound	Refers to Pratt (1982)	Spongiostromate accretion with birdseyes and fenestrae
Hadding, 1959	Silurian (Wenlock), Gotland	Spongiostroma: concentric layered balls of dusty flocculent or diffusely nodular algal mass, including Girvanella, Hedströmia & shell frags; porous structure filled with calcite cement. An irregular network of dark algal portions & light clear interstitial calcite	Formed by rolling around in soft mud. V shallow marine conditions	Spongiostroma made of what are now called calcimicrobes and cements. Sponges not mentioned.
Larmagnat and Neuweiler, 2015	Ordovician bryozoan mound	Microbial tunneling, keratose sponge	Problematic	Referenced in Lee & Riding (2021) as “microtubules of keratose sponges or fungi”
Shen and Neuweiler, 2018	Ordovician sponge mound	Fig, 11, 17: AM-3; metazoan calcified ECM, (keratose sponge), invertebrate anchoring apparatus	Calcified ECM, Problematic	Not clear, only very small contribution to overall rock fabric
Park et al., 2017	U. Ordovician sponges in shells	Networks in micrite infilling in shell and corals; but also peloids in shells	Hard to see how these are sponges	Peloids in shells do not resemble spiculate sponges; networks in infillings of shells and corals not clear origin
Kwon et al., 2012	L. Ordovician tetradiid-siliceous sponge reefs	Spicule networks that laterally grade into irregular pockets of peloidal fabric containing spicules	Siliceous sponges in various states of preservation	Re-interpreted in Lee & Riding (2021) as keratose sponge
Park et al., 2015	U. Ordovician (Xiazhen Fm, SE China)	Vermicular structures described as spicules, occurring as incomplete sponges in discrete masses in micritic bedded limestones	Non-lithistid spicular demosponges	Not described as keratose sponges, but spicular sponges. Does not provide criteria for distinction.
Li et al., 2017b	M. Ordovician calathiid reefs,	Claim lithistid sponges (Fig. 9)	Maybe lithistid sponge	Poorly illustrated as lithistid sponges, but

	with some other sponges			certainly different from any networks
Desrochers and James, 1989	M. Ordovician bioherms	Their Fig. 7f: Vermiform microstructure: cryptalgal crust <i>versus</i> sponge remains	Poorly preserved spicular network ?	Vermiform to spiculiferous microtexture of others
Lee et al., 2016	M. Ordovician	Beautiful pictures Fig. 4 & 5, of peloidal and network structures, that are all described as sponges	Peloidal images look like peloids; network images could be clotted micrite	Very nice photos, but verification of sponges not provided.
Hong et al., 2017	M. Ordovician stromatoporoid frameworks	Sponge spicule masses in sediment in metazoan framework	Maybe these are sponges	Have similarity to networks shown by Kershaw et al. 2021.
Hong et al., 2018	M Ordovician	Rather indistinct network-looking structures in micrite infillings in borings in stromatoporoids	Described as sponges	Really cannot be clear about what these are
Kapp, 1975	M. Ordovician stromatoporoid mound	Fig.3: Lenticular crusts with tubules (straight curled, branching); birdseyes, (touching) vugs.	Algal crusts with molds of filaments	LM-microbialite of Bourillot et al., 2020
Kapp, 1975	Middle Ordovician stromatoporoid mound	Fig.7: Microboring in stromatoporoid	Microboring	Microendoliths
Ross et al., 1975	M. Ordovician mud-mound	Fig. 23, 25, 27; pelletoid texture, meshwork below sponges, algal borings, cement fabric	Polygenic; to be resolved only very locally	Spongiostromata, spongiform geopetals, mikroendoliths, intergranular cement
Pratt and James, 1989	L. Ordovician thrombolite reefs	Their Fig. 8 and 9. Spongiform, vermiform and tubiform microstructure, incl. burrows in lime mudstone	Refers <i>pro parte</i> to <i>Spongiostroma</i> (cryptalgal origin)	Complex co-occurrence of a variety of microstructures set well apart from sponge remains
Liu et al., 1997	L. Ordovician small-scale reefs	Moderately diverse assemblage of demosponges (minor hexactinellids)	Spicule-rich, mottled matrix (Fig. 6-1; 6-3)	Referenced by Lee & Riding (2021) as "not-recognized" keratose sponges
Adachi et al., 2009	L. Ordovician reefs	Microbial-lithistid sponge-receptaculitid boundstones	Spicule-rich, mottled matrix (Fig. 5D)	Referenced by Lee & Riding (2021) as "not-recognized" keratose sponges
John and Eby, 1978	L. Ordovician	Stromatolites with spar-filled tubules or borings; spongy meso- to microfabric	Cryptalgal laminites	LM-microbialite of Bourillot et al., 2020
Li et al., 2019a	L Ordovician	Some poorly illustrated clotted/network structures considered to be "sponge remains"	Sponge remains	No verification of sponges

Hong et al., 2015	L. Ordovician (Dumugol Fm, Korea)	Sponges: Archaeoscyphia definite sponge; non-anthaspidellid spiculate sponges previously not reported from L. Ordn reefs before. NOTE: they call all these as SILICEOUS sponges, but replaced by calcite (p.78,RH,Line2)	Earliest Ordn sponges in reefs; siliceous spiculate sponges (even though preserved as calcite).	Assumes spicules were siliceous & replaced by calcite. Not mentioned keratose (keratose does not appear in the paper).
Li et al., 2017a	L. Ordovician reefs	Lithistid (Fig. 3) and keratose (Fig. 4) sponges are both identified here	Seem to be no criteria for recognition of either kind of sponge	
Hong et al. 2014	L. Ordovician microbial-siliceous sponge reefs	Spiculate sponges in cryptic position	Siliceous sponges at various states of preservation	Re-interpreted in Lee & Riding (2021) as keratose sponge
Li et al., 2015	L. Ordovician calathid reefs	Figs. 5&6 show pictures of calathids with rather dark images of areas labelled as lithistid sponge	Calathiid and lithistid sponges	Too poorly illustrated to make any objective conclusion about whether there are sponges here or not
Li et al., 2019b	L. Ordovician	States that sponge-microbe associations developed in Cambrian; describes “anastomosing microtubules” as “probably keratose sponges”	Probably keratose sponges	Note that this is a conference abstract with one figure. No verification of sponges
Lee and Riding, 2021b	U. Cambrian to L. Ordovician	Names keratose sponges as keratolite, and illustrates interpreted consortia between keratolite and stromatolite carbonate.	Consortia of keratose sponge and stromatolite	No verification of keratose sponge. Contains numerous references to keratose sponges, but those references do not verify they are sponges.
Pham and Lee, 2020	Tremadoc Mungok Fm, Korea	Vermicular structures, described as keratose sponges without any justification. Also spiculate sponges present (more believable)	Keratose sponges	As other papers, there is no verification of sponges here.
Lee and Riding, 2020	U. Cambrian	“Cryptozoon” - sponge-microbial consortium. Claims keratose sponge is part of the consortium	Maybe sponge but not verified	
Lee and Riding, 2021a	U. Cambrian	Cryptozoon redefined as consortium of keratose sponge and microbial carbonate in approximately equal proportions.	Consortium of keratose sponge and microbial carbonate	Page 5 notes that keratose sponges may be misidentified as lithistids, does attempt criteria for

		Illustrations of networks that may be keratose sponges. Fig. 9 compares Cambrian lithistids with vermiform networks as indication of difference between lithistids and keratose sponges.		discrimination, but not very convincing; it partly depends on the interpretation of keratose sponges being correct, which is not verified. Thus no criteria offered for distinguishing between keratose sponges and other possible interpretations.
Kennard et al., 1989	Mid-Cambrian thrombolite-stromatolite bioherm	Complex fabric of mesoclots, stromatoids and marine cement.. Fig.6: finely clotted fabric	Network of calcified coccoid microbial colonies	Spongistromate to vermiform microtexture of others (their Fig. 6)
Turner, 2021	Neoproterozoic in Canada	Vermicular structures as calcite spar infill in micrite matrix; interpreted as “possible keratose sponges”	Possible keratose sponges	Problem is that no alternatives are offered, too much preference for a sponge interpretation. Also rocks too old to be considered verifiable sponges?

301 **Table References**

- 302 Adachi, N., Ezaki, Y., Liu, J., Cao, J. (2009) Early Ordovician reef construction in Anhui  
303 Province, South China: A geobiological transition from microbial- to metazoan-dominant  
304 reefs. *Sedimentary Geology*, **220**, 1–11.
- 305 Adachi, N., Asada, Y., Ezaki, Y., Liu, J.B. (2017) Stromatolites near the Permian-Triassic  
306 boundary in Chongyang, Hubei Province, South China: a geobiological window into  
307 Palaeo-oceanic fluctuations following the end-Permian extinction. *Palaeogeography,*  
308 *Palaeoclimatology, Palaeoecology*, **475**, 57–69.
- 309 Baud, A., Richoz, S., Brandner, R., Krystyn, L., Heindel, K., Mohtat, T., Mohtat-Aghai, P.,  
310 Horacek, M. (2021) Sponge takeover from end-Permian mass extinction to early Induan  
311 time: records in central Iran microbial buildups. *Frontiers in Earth Science*, **9**, 586210.
- 312 Brayard, A., Vennin, E., Olivier, N., Bylund, K.G., Jenks, J., Stephen, D.A., Bucher, H.,  
313 Hofmann, R., Goudemand, N., Escarguel, G. (2011) Transient metazoan reefs in the  
314 aftermath of the end-Permian mass extinction. *Nature Geoscience*, **4**, 694–697.
- 315 Brayard, A., Krumenacker, L.J., Botting, J.P., Jenks, J.F., Bylund, K.G., Fara, E., Vennin,  
316 E., Olivier, N., Goudemand, N., Saucède, T., Charbonnier, S., Romano, C., Doguzhaeva,  
317 L., Thuy, B., Hautmann, M., Stephen, D.A., Thomazo, C., Escarguel, G. (2017)  
318 Unexpected Early Triassic marine ecosystem and the rise of the Modern evolutionary  
319 fauna. *Science Advances*, **3**, e1602159.
- 320 Cayeux, L., (1935) *Les Roches sédimentaires de France: roches*  
321 *carbonatées*. Paris. Masson et Cie.
- 322 Clough, J.G., Blodgett, R.B. (1989) Silurian-Devonian Algal Reef Mound Complex of  
323 Southwest Alaska. In: Geldsetzer, H.H.J., James, N.P. and Tebbutt, G.E. (eds), *Reefs:*  
324 *Canada and Adjacent Area*, Canadian Society of Petroleum Geologists Memoir, **13**, 404–  
325 407.
- 326 Desrochers, A, James, N.P. (1989) Middle Ordovician (Chazyan) bioherms and  
327 biostromes of the Mingan Islands, Quebec. In: Geldsetzer, H.H.J., James, N.P. and

- 1328 Tebbutt, G.E. (eds), *Reefs: Canada and Adjacent Area*, Canadian Society of Petroleum  
1329 Geologists Memoir, **13**, 183–19.
- 1330 Friesenbichler, E., Richoz, S., Baud, A., Krystyn, L., Sahakyan, L., Vardanyan, S.,  
1331 Peckmann, J., Reitner, J., Heindel, K. (2018) Sponge-microbial build-ups from the  
1332 lowermost Triassic Chanakhchi section in southern Armenia: Microfacies and stable  
1333 carbon isotopes. *Palaeogeography, Palaeoclimatology, Palaeoecology*, **490**, 653–672.
- 1334 Gürich, G. (1906). Les spongiostromides du Viséen de la Province de Namur. *Memoirs of*  
1335 *the Royal Belgian Museum of Natural Sciences*, **3**, 1–55.
- 1336 Hadding, A., (1959) Silurian algal limestones of Gotland. *Lunds. Univ. Arsskrift*, **56**, 1-25.
- 1337 Heindel, K., Foster, W.J., Richoz, S., Birgel, D., Roden, V.J., Baud, A., Brandner, R.,  
1338 Krystyn, L., Mohtat, T., Koşun, E., Twitchett, R.J., Reitner, J., Peckmann, J. (2018) The  
1339 formation of microbial-metazoan bioherms and biostromes following the latest Permian  
1340 mass extinction. *Gondwana Research*, **61**, 187–202.
- 1341 Hong, J., Choh, S.-J., Lee, D.-J. (2014) Tales from the crypt: Early adaptation of  
1342 cryptobiontic sessile metazoans. *Palaios*, **29**, 95–100.
- 1343 Hong, J., Choh, S.-J., Lee, D.-J. (2015) Untangling intricate microbial–sponge frameworks:  
1344 the contributions of sponges to Early Ordovician reefs. *Sedimentary Geology*, **318**, 75–  
1345 84.
- 1346 Hong, J., Choh, S.-J., Park, J., Lee, D.-J. (2017) Construction of the earliest  
1347 stromatoporoid framework: Labechiid reefs from the Middle Ordovician of Korea.  
1348 *Palaeogeography, Palaeoclimatology, Palaeoecology*, **470**, 54–62.
- 1349 Hong, J., Oh, J.-R., Lee, J.-H., Choh, S.-J., Lee, D.-J. (2018) The earliest evolutionary link  
1350 of metazoan bioconstruction: Laminar stromatoporoid–bryozoan reefs from the Middle  
1351 Ordovician of Korea. *Palaeogeography, Palaeoclimatology, Palaeoecology*, **492**, 126–  
1352 133.
- 1353 John, J.W.St., Eby, D.E. (1978) Peritidal carbonates and evidence for vanished evaporites  
1354 in the Lower Ordovician Cool Creek Formation–Arbuckle Mountains, Oklahoma. *Gulf*  
1355 *Coast Association of Geological Societies Transactions*, **28**, 589–599.
- 1356 Kaisin, F. (1922) Les roches du Dinantien de Belgique. *Comptes-rendus du Congrès*  
1357 *géologique international (Belgique)*, XIII<sup>o</sup> Session, Fasc. III, 1237-1269.
- 1358 Kaisin, F. (1925) La formation des calcaires oolithiques de Belgique. *Annales de la Société*  
1359 *scientifique de Bruxelles*, 44, 3, 362-365.
- 1360 Kapp, U.S. (1975) Paleocology of Middle Ordovician stromatoporoid mounds in Vermont.  
1361 *Lethaia*, **8**, 195–207.
- 1362 Kennard, J.M., Chow, N., James, N.P. (1989) Thrombolite-stromatolite bioherm, Middle  
1363 Cambrian, Port Au Port Peninsula, western Newfoundland. In: Geldsetzer, H.H.J.,  
1364 James, N.P. and Tebbutt, G.E. (eds), *Reefs: Canada and Adjacent Area*, Canadian  
1365 Society of Petroleum Geologists Memoir, **13**, 151–155.
- 1366 Kwon, S.-W., Park, J., Choh, S.-J., Lee, D.-C., Lee, D.-J. (2012) Tetradiid-siliceous sponge  
1367 patch reefs from the Xiazhen Formation (late Katian), southeast China: A new Late  
1368 Ordovician reef association. *Sedimentary Geology*, **267**, 15–24.
- 1369 Larmagnat, S., Neuweiler, F. (2015) Taphonomic filtering in Ordovician bryozoan  
1370 carbonate mounds, Trenton Group, Montmorency Falls, Quebec, Canada.  
1371 *Palaios*, **30**, 169–180.
- 1372 Lee, J.-H. and Riding, R. (2020) The ‘classic stromatolite’ *Cryptozoön* is a keratose  
1373 sponge-microbial consortium. *Geobiology*, **19**, 189-198. DOI: 10.1111/gbi.12422.
- 1374 Lee, J.-H., Riding, R. (2021a) The ‘classic stromatolite’ *Cryptozoön* is a keratose sponge-  
1375 microbial consortium. *Geobiology*, **19**, 189–198.
- 1376 Lee, J.-H., Riding, R. (2021b) Keratolite–stromatolite consortia mimic domical and  
1377 branched columnar stromatolites. *Palaeogeography, Palaeoclimatology,*  
1378 *Palaeoecology*, **571**, 110288.

- 379 Lee, J.-H., Woo, J., Lee, D.-J. (2016) The earliest reef-building anthaspidellid sponge  
380 *Rankenella zhangxianensis* n. sp. from the Zhangxia Formation (Cambrian Series 3),  
381 Shandong Province, China. *Journal of Paleontology*, **90**, 1–9.
- 382 Lees, A., (1964) The structure and origin of the Waulsortian (Lower Carboniferous) “reefs”  
383 of west-central Eire. *Philosophical Transactions of the Royal Society B*, **247**: 483–531.
- 384 Li, Q., Li, Y., Wang, J., Kiessling, W. (2015) Early Ordovician lithistid sponge–  
385 *Calathium* reefs on the Yangtze Platform and their paleoceanographic implications.  
386 *Palaeogeography, Palaeoclimatology, Palaeoecology*, **425**, 84–96.
- 387 Li, Q., Li, Y., Kiessling, W. (2017a) The oldest labechiid stromatoporoids from intraskeletal  
388 crypts in lithistid sponge-*Calathium* reefs. *Lethaia*, **50**, 140–148.
- 389 Li, Q., Li, Y., Zhang, Y., Munnecke, A. (2017b) Dissecting *Calathium*-microbial  
390 frameworks: The significance of calathids for the Middle Ordovician reefs in the Tarim  
391 Basin, northwestern China. *Palaeogeography, Palaeoclimatology, Palaeoecology*, **474**,  
392 66–78.
- 393 Li, Q.-J., Sone, M., Lehnert, O., Na, L. (2019a) Early Ordovician sponge-bearing  
394 microbialites from Peninsular Malaysia: The initial rise of metazoans in reefs.  
395 *Palaeoworld*, **28**, 80–95.
- 396 Li, Q.J., Agematsu, S., Na, L., Sardud, A.A. (2019b) Stromatolite abundance anomaly in  
397 Early Ordovician: the rise of sponge-microbial association? In:  
398 Obut, O.T., Sennikov, N.V. and Kipriyanova T.P. (eds), 13th International Symposium on  
399 the Ordovician System, Novosibirsk, 113–114.
- 400 Liu, B., Rigby, J.K., Jiang, Y., Zhu, Z. (1997) Lower Ordovician lithistid sponges from the  
401 eastern Yangtze Gorge Area, Hubei, China. *Journal of Paleontology*, **71**, 194–207.
- 402 Luo, C., Reitner, J. (2014) First report of fossil “keratose” demosponges in Phanerozoic  
403 carbonates: Preservation and 3-D reconstruction. *Naturwissenschaften*, **101**, 467–477.
- 404 Luo, C. (2015) “Keratose” Sponge Fossils and Microbialites: A Geobiological Contribution  
405 to the Understanding of Metazoan Origin. Ph.D. Thesis, Georg-August-Universität  
406 Göttingen, 151 pp.
- 407 Luo, C., Reitner, J. (2016) ‘Stromatolites’ built by sponges and microbes—a new type of  
408 Phanerozoic bioconstruction. *Lethaia*, **49**, 555–570.
- 409 Monty, C., (1981) *Phanerozoic Stromatolites*. Springer-Verlag, Berlin Heidelberg, 252 pp.
- 410 Park, J., Lee, J.-H., Hong, J., Choh, S.-J., Lee, D.-C., Lee, D.-J. (2015) An Upper  
411 Ordovician sponge-bearing micritic limestone and implication for early Palaeozoic  
412 carbonate successions. *Sedimentary Geology*, **319**, 124–133.
- 413 Park, J., Lee, J.-H., Hong, J., Choh, S.-J., Lee, D.-C., Lee, D.-J. (2017) Crouching shells,  
414 hidden sponges: Unusual Late Ordovician cavities containing sponges. *Sedimentary  
415 Geology*, **347**, 1–9.
- 416 Pham, D., Lee, J.-H (2020) Keratose sponge–microbial carbonate consortium in the  
417 columnar “stromatolites” and “thrombolite” mounds from the Lower Ordovician Mungok  
418 Formation, Yeongwol, Korea. In:  
419 Rasmussen, C.M.Ø., Stigall, A.L., Nielsen, A.T., Stouge, S. and  
420 Schovsbo, N.H. (eds.), *Zooming in on the GOBE: 2020 Virtual Annual Meeting of  
421 IGCP653*, Geological Survey of Denmark and Greenland, p. 37.
- 422 Pratt, B.R., James, N.P. (1989) Early Ordovician thrombolite reefs, St. George Group,  
423 western Newfoundland. In: Geldsetzer, H.H.J., James, N.P. and Tebbutt, G.E. (eds),  
424 *Reefs: Canada and Adjacent Area*, Canadian Society of Petroleum Geologists Memoir,  
425 **13**, 231–240.
- 426 Pratt, B.R. (1982) Stromatolitic framework of carbonate mud-mounds. *Journal of  
427 Sedimentary Petrology*, **52**, 1203–1227.
- 428 Rodríguez-Martínez, M., Reitner, J., Mas, R. (2010) Micro-framework reconstruction from  
429 peloidal-dominated mud mounds (Viséan, SW Spain). *Facies*, **56**, 139–156.

- 430 Rodríguez-Martínez, M., Moreno-González, I., Mas, R., Reitner, J. (2012)  
431 Paleoenvironmental reconstruction of microbial mud mound derived boulders from  
432 gravity-flow polymictic megabreccias (Visean, SW Spain). *Sedimentary Geology*, **263–**  
433 **264**, 157–173.
- 434 Ross Jr., R.J., Jaanusson, V., Friedman, I. (1975) Lithology and origin of Middle  
435 Ordovician calcareous mudmound at Meiklejohn Peak, Southern Nevada. *United States*  
436 *Geological Survey Professional Paper*, **871**, 48 pp.
- 437 Schwarzacher, W. (1961) Petrology and Structure of Some Lower Carboniferous Reefs in  
438 Northwestern Ireland. *American Association of Petroleum Geologists Bulletin*, **45**, 1481–  
439 1503.
- 440 Shen, Y., Neuweiler, F. (2018) Questioning the microbial origin of automicrite in Ordovician  
441 calathid-demosponge carbonate mounds. *Sedimentology*, **65**, 303–333.
- 442 Stock, C.W., Sandberg, C.A. (2019) Latest Devonian (Famennian, *expansa* Zone)  
443 conodonts and sponge-microbe symbionts in Pinyon Peak Limestone, Star Range,  
444 southwestern Utah, lead to reevaluation of global Dasberg Event. *Palaeogeography,*  
445 *Palaeoclimatology, Palaeoecology*, **534**, 109271.
- 446 Tsien, H.H. (1985) Algal-bacterial origin of micrites in mud mounds. In: Toomey, D.F. and  
447 Nitecki, M.H. (eds), *Paleoalgology: Contemporary Research and Applications*, Springer-  
448 Verlag Berlin Heidelberg, 290–296.
- 449 Turner, E.C. (2021) Possible poriferan body fossils in early Neoproterozoic microbial reefs.  
450 *Nature*, **596**, 87–91.
- 451 Wolf, K.H. (1965a) Petrogenesis and palaeoenvironment of Devonian algal limestones of  
452 New South Wales. *Sedimentology*, **4**, 113–178.
- 453 Wolf, K.H. (1965b) Gradational Sedimentary Products of Calcareous Algae.  
454 *Sedimentology*, **5**, 1–37.
- 455 Zhou, K., Pratt, B.R. (2019) Composition and origin of stromatolite-bearing mud-mounds  
456 (Upper Devonian, Frasnian), southern Rocky Mountains, western Canada.  
457 *Sedimentology*, **66**, 2455–2489.  
458